Fas-threshold Signalling in MSCs Promotes Pancreatic Cancer Progression and Metastasis

Andrea Mohr[1,*], Tianyuan Chu[1], Christopher T. Clarkson[2], Greg N. Brooke[3], Vladimir B. Teif[2], Ralf M. Zwacka[1,*]

[1]School of Life Sciences, Protein Structure and Mechanism of Disease Group, Cancer and Stem Cell Biology Laboratory, University of Essex, Colchester, CO4 3SQ, UK
[2]School of Life Sciences, Genomics and Computational Biology Group, Gene Regulation Laboratory, University of Essex, Colchester, CO4 3SQ, UK
[3]School of Life Sciences, Protein Structure and Mechanism of Disease Group, Molecular Oncology Laboratory, University of Essex, Colchester, CO4 3SQ, UK

Running title: Tumours stimulate MSC-proliferation via Fas signalling

Corresponding author:
*correspondence: amohr@essex.ac.uk; rzwacka@essex.ac.uk

Andrea Mohr and Ralf Michael Zwacka
University of Essex
School of Life Sciences
Colchester
CO4 3SQ
United Kingdom

Keywords: MSC-proliferation, pancreatic cancer, FasL, CCL2, IL1

Abstract

Mesenchymal stem cells (MSCs) belong to the tumour microenvironment and have been implicated in tumour progression. We found that the number of MSCs significantly increased in tumour-burdened mice driven by Fas-threshold signalling. Consequently, MSCs lacking Fas lost their ability to induce metastasis development in a pancreatic cancer model. Mixing of MSCs with pancreatic cancer cells led to sustained production of the pro-metastatic cytokines CCL2 and IL6 by the stem cells. The levels of these cytokines were dependent on the number of MSCs, linking Fas-mediated MSC-proliferation to their capacity to promote tumour progression. Furthermore, we discovered that CCL2 and IL6 were induced by pancreatic cancer cell-derived IL1. Importantly, analysis of patient transcriptomic data revealed that high FasL expression correlates with high levels of MSC markers as well as increased IL6 and CCL2 levels in pancreatic tumours. Moreover, both FasL and CCL2 are linked to elevated levels of markers specific for monocytes known to possess further pro-metastatic activities. These results confirm our experimental findings of a FasL-MSC-IL1-CCL2/IL6 axis in pancreatic cancer and highlights the role of MSCs in tumour progression.

1. Introduction

FasL has recently been shown to induce proliferation of human mesenchymal stem cells (MSCs) *in vitro* [1]. Although MSCs were found to proliferate in the tumour microenvironment (TME) [2], a direct connection between increased MSC numbers and FasL-induced proliferation has not been established *in-vivo*. Furthermore, it is not clear as to whether this increase in MSCs might be linked to their pro-metastatic activity. FasL, also known as CD95L, is commonly known for its pro-apoptotic function via FADD and Caspase-8 [3, 4]. However, more recently, it was shown that FasL can also trigger non-apoptotic/non-canonical pathways [5-10]. Several reports have described this as Fas-threshold signalling, in which low concentrations of FasL promote survival signalling and growth [11-14]. In patient samples, FasL has been found at elevated levels in various cancer types [15-26], and has been associated with tumour progression [27-37]. Most of this work, however, has focused on Fas/FasL signalling in cancer cells without consideration of the more complex cellular interactions and regulatory circuits between malignant and non-malignant cells, such as MSCs, present in the TME [38].

MSCs are initially recruited to the tumour from the bone marrow or other tissues during tumourigenesis [39-41], where they can promote cancer cell dissemination and the development of metastatic lesions [42, 43]. One of the factors involved in this process, identified in breast cancer metastasis, is the Chemokine (C-C motif) ligand 5 (CCL5), which is also known as RANTES (Regulated on activation, normal T cell expressed and secreted) [43]. CCL5 was shown to be induced by cancer cell-derived osteopontin (OPN) in MSCs [44]. However, CCL5 did not appear to regulate the MSC-induced metastasis of all breast cancer models investigated [43], and its role in other cancer types is also not yet

clear. Thus, it seems likely that additional and yet to be identified factors and mechanisms will have critical roles in MSC-driven tumour progression. Pancreatic cancer is characterised by a pronounced stromal desmoplastic reaction, in which tumour-infiltrating MSCs and carcinoma-associated fibroblasts (CAFs) derived from MSCs become a major component of the TME [45-48]. In the pancreatic cancer TME, MSCs were shown to contribute to angiogenesis and thereby potentially lead to tumour progression by VEGF expression [49]. In addition, MSC-derived myofibroblasts play important roles in regulating epithelial-mesenchymal transition (EMT) and maintaining tumour-initiating stem cells of pancreatic cancer cells by an intermediating Notch signal [50]. Another study reported that pancreatic cancer-induced Amphiregurin (AREG) expression in MSCs plays a critical role in cancer invasion [51]. A strong co-localisation of the soluble ligand AREG and its receptor EGFR in the invasive front, where MSCs are also present, suggests that secreted AREG stimulates the cancer cells to trigger local invasion [51]. Furthermore, primary patient pancreatic tumour samples and low-passage human pancreatic CAF cultures were found to contain a unique population of cancer-associated MSCs which markedly enhance the growth, invasion, and metastatic potential of pancreatic cancer cells by secretion of the cytokine GM-CSF [52]. To study the link between cancer-induced MSC proliferation and their pro-metastatic behaviour, we examined the action of FasL on MSCs and their crosstalk with pancreatic cancer cells.

2. Materials and methods

2.1 Cell culture and reagents

The colorectal carcinoma cell lines HT29 (ATCC, Manassas, VA, USA) and Colo205 (ATCC) were cultured in RPMI (Lonza, Basel, Switzerland) and in McCoy's 5A (Lonza), respectively. The prostate cancer cell lines, LNCaP (ATCC) and PC3 (ATCC), were cultured in RPMI medium. The breast cancer cell lines, MDA-MB-231 (ATCC) and MCF7 (ATCC), were cultured in DMEM (Lonza) and in EMEM (Lonza) medium, respectively. The pancreatic cancer cells PancTu1, Jurkat cells (both obtained from Prof Simone Fulda), AsPC1 (ATCC) and BxPC3 (ATCC) cells were cultured in RPMI medium, while MiaPaCa2 (ATCC) and HEK293 (ATCC) cells were grown in DMEM medium. All media were supplemented with 10% foetal bovine serum (FBS) (Thermo Fisher Scientific, Waltham, MA, USA), 100 U/ml penicillin and 100 µg/ml streptomycin. The PancTu1 cells are genetically altered in K-ras, p53 and p16 genes. The histology and tumour stage are PDAC and G3, respectively.

Human bone marrow derived MSCs were from Lonza, umbilical cord derived MSCs were purchased from Promocell (Heidelberg, Germany), and human adipose derived stem cells were acquired from Amsbio (Cambridge, MA, USA). Human MSCs were cultured in StemMACS MSC Expansion Medium (Miltenyi Biotec, Bergisch Gladbach, Germany). Murine MSCs and LPR-MSCs were isolated and cultured, as previously described [42, 53, 54].

The following inhibitors, all purchased from Stratech, Ely, UK, were used: STAT3i (C188-9), PI3Ki (AZD8186 and BYL719), ERKi (PD0325901), p38i (R1503), NF-kBi (Bay11), JNKi (SP600125). The pan-caspase inhibitor zVAD was bought from Enzo (Farmingdale,

NY, USA). The following cytokines were ordered from Peprotech (Rocky Hill, NJ, USA): IGF1, IL1α, IL1β, OSM, PDGF and VEGF. TRAIL, IL6, CCL2, anti-CCL2 antibody, human IL6Rα and human gp130 were purchased from Biotechne (Minneapolis, MN, USA), FasL from Enzo, multimeric-FasL and anti-APO-1-3 from AdipoGen Life Sciences (San Diego, CA, USA). IL1RA and the FasL neutralising antibody NOK-1 were purchased from Biolegend (San Diego, CA, USA), while the anti-IL6 antibody was bought from Diaclone (Besancon, France). The FasL is produced in HEK 293 cells and the extracellular domain (aa 103-281) is fused at the N-terminus to a linker peptide (26 aa) and a FLAG-tag. The anti-APO-1-3 is an anti-human Fas mouse IgG3 agonistic monoclonal antibody purified from concentrated hybridoma tissue culture supernatant. The multimeric-FasL is the human FasL (aa 139-281) fused at the N-terminus to mouse ACRP30headless (aa 18-111) and a FLAG-tag. It is a high activity FasL in which two trimeric FasL complexes are artificially linked via the ACRP30 domain.

2.2 Animal studies

Ten-week-old female CD1 nu/nu mice (Charles River) were subcutaneously injected with 5×10^6 MDA-MB-231 or PancTu1 cells in 200 µl PBS under the lateral skin of the right leg. When tumours were palpable, the animals were injected intravenously with 1×10^5 Chloromethyl-dialkylcarbocyanine (CM-Dil; Thermo Fisher Scientific) labelled MSCs. For the analysis of the tissue distribution of the MSCs and their effects on metastasis formation inguinal, axillary, mesenteric and paraaortic lymph nodes, liver, spleen, kidney, lungs and tumours were fixed in 10% neutral buffered formalin. In addition, tibia and femur, and vertebra of each animal were formalin fixed, followed by decalcification with

a solution of 8% formic acid/8% HCl prior to tissue processing and paraffin embedding. For histopathological analyses, four μm-paraffin sections were stained with Haematoxylin and Eosin (H&E) and examined using light microscopy. All animal studies were carried out in accordance with the EU Directive 2010/63/EU for animal experiments in line with national laws and covered by license from the Irish government.

To detect MSCs *in vivo*, they were loaded with four μg/ml CM-Dil in pre-warmed PBS for 15 minutes at 37° C followed by an incubation for 15 min at 4°C. The cells were washed with PBS, resuspended in their normal growth medium, and subsequently cultured for 16 hours before they were used. For quantification of MSC bio-distribution, four μm-paraffin sections were deparaffinised and rehydrated, washed in PBS, followed by incubation for ten minutes with DAPI, and mounted in fluoromount solution for the detection of fluorescent cells under a microscope. 15 randomly chosen fields/organ of each animal were numbered.

2.3 Cell surface staining

$1x10^6$ cells were incubated with fluorochrome conjugated antibodies for 15 minutes on ice in the dark**.** Before flow cytometric analyses, the cells were washed with PBS containing 1% BSA. The following PE-conjugated antibodies were used for cell surface staining: human CD95 (DX2) and mouse CD95 (SA367H8). PE-conjugated Mouse IgG1κ was used as the isotype control. All antibodies used were purchased from BioLegend and were used at a concentration of 0.2 μg/10^6 cells.

2.4 Cell growth assays

MSCs were plated at a density of $1x10^4$ in a 24-well plate. After 24 hours, medium was changed to DMEM containing 1% FCS. 12 hours later, the cells were treated with 0.2 ng/ml FasL, 0.2 ng/ml multimeric-FasL, and 0.2 ng/ml anti-APO-1-3, respectively, or at concentrations indicated in the figure legends. As control, cells were treated with 0.2 ng/ml TRAIL. JNKi, p38i, ERKi were added at a concentration of 1 µM, 20 minutes before FasL was added. To measure cell numbers, cells were detached with trypsin solution and counted using a haemocytometer. Crystal violet staining was performed seven days later, as previously described [55].

2.5 Apoptosis assays

MSCs were plated at a density of $5x10^4$ in a 24-well plate. After 24 hours, cells were treated with FasL, multimeric-FasL, or anti-APO-1-3. Apoptosis was measured according to Nicoletti et al. [56]. Cells were harvested and washed once with PBS after 24 hours of treatment. They were resuspended in hypotonic fluorochrome solution containing 50 μg/ml propidium iodide, 0.1% sodium citrate, and 0.1% Triton-X100. After incubation at 4°C for two hours, cells were analysed by flow cytometry.

Apoptosis in Jurkat cells was measured using the Nicoletti-method, as described above. For this, Jurkat cells were mixed with cell supernatants (from 10^4 cells cultured for 48 hours) or cells (10^4) for 48 hours before apoptosis was measured.

2.6 Western blot

MSCs were serum starved for 24 hours, before 0.2 ng/ml FasL was added. Cells were harvested at the indicated time points. To analyse the effects of tumour cell supernatants on MSCs, stem cells were seeded, and 24 hours later, the growth medium was replaced with cell supernatant for the indicated time-points. For caspase western blots hMSCs were treated with 5 ng/ml FasL or 5 ng/ml multimeric-FasL in regular growth medium for 24 hours. SDS-PAGE and transfer onto PVDF membranes were performed as described previously [57]. The following primary antibodies were used: anti-phospho-SAPK/JNK (Cell Signaling Technology, Danvers, MA, USA), anti-total-SAPK/JNK (Cell Signaling Technology), anti-phospho-p38 MAPK (Cell Signaling Technology), anti-total-p38 MAPK (Cell Signaling Technology), anti-phospho-ERK (Cell Signaling Technology), anti-total-ERK (Cell Signaling Technology), anti-CD95 (Santa Cruz Biotechnology, Dallas, TX, USA), anti-IκBα (Cell Signaling Technology), anti-caspase-3 (Biotechne), anti-caspase-8 (Cell Signaling Technology), anti-vimentin (BioLegend) and anti-CuZnSOD (Binding Site, Birmingham, UK). Peroxidase-conjugated secondary antibodies were anti-rabbit and anti-goat sourced from Santa Cruz. All antibodies were diluted to a working concentration of 1:1000. Proteins were visualised using ECL and a Fusion FX Chemidoc Imager (Vilber, Collégien, France).

2.7 NF-κB reporter assay

MSCs were seeded in 12-well plates. Next day, cells were transduced with adenovirus containing an NF-κB-firefly-luciferase vector (Vector Biolabs, Malvern, PA, USA) at an MOI of 200. 24 hours after transduction, the cells were pre-treated with 1 μM NF-κB

inhibitor or IL1RA (4 μg/ml) for 20 minutes before tumour cell supernatant was added. 24 hours post treatment, cells were lysed in passive lysis buffer (Promega, Madison, WI, USA). Luciferase activity was measured using a luminometer.

2.8 ELISA

$1x10^4$ tumour cells were either mixed with varying numbers of MSCs ($1x10^4$ (1:1) or $1x10^3$ MSCs (1:10)) or treated with tumour cell supernatants for two days. To test for cytokine induction, $1x10^4$ cells were cultured and subsequently treated with 0.2 ng/ml of the respective death ligands, 50 ng/ml of IGF1, IL1α, IL1β, OSM, PDGF-BB, TPO or VEGF-A, 2.5 μg/ml sIL6Rα, 2.5 μg/ml IgG1κ, 2.5 μg/ml anti-IL6, 2.5 μM STAT3i, different PI3K inhibitors (PI3Ki-1: AZD8186, PI3Ki-2: BYL719) and the NK-κB inhibitor at concentrations of 1 μM, 4 μg/ml IL1RA or 2.5 μg/ml gp130-Fc for 48 hours. Supernatants were removed and cleared by centrifugation. The human and murine cytokines IL6, CCL2 and CCL5 levels were determined by DuoSet ELISA (Biotechne), according to manufacturer's instructions.

To analyse the sustained secretion of CCL2 and IL6 by MSCs, supernatants from PancTu1 cells were applied to $1x10^4$ MSCs. The medium was changed to fresh medium at days three and six. Cells without medium change served as control. 50 μl of media were taken for analysis every three days. The 50 μl taken for experiments were replaced with fresh medium. For the measurement of sIL6R, IL1RA, IL1α and IL1β, the supernatant was taken from cells cultured for three days. The volumes of supernatants used for these ELISAs were adjusted to the respective cell number.

The FasL ELISA (Diaclone) was carried out according to the manufacturer's instructions. Cell supernatants of 10^4 cells cultured for 48 hours were harvested and cleared by centrifugation before being applied to the coated ELISA plates. HEK293 cells transfected with a human FasL expression construct (InvivoGen, Toulouse, France) were used as positive control. The transfection was carried out with FuGene HD (Promega).

2.9 Cytokine Array

Supernatants were taken from hMSCs and tumour cells at a ratio of one MSC to ten tumour cells and cytokine levels were compared to the MSCs and tumour cells cultured separately. The supernatants were diluted 3.5-fold and applied to human cytokine antibody arrays III (RayBiotech, Norcross, GA, USA) according to the manufacturer's instructions. Each cytokine signal was normalised to its internal control and the fold change calculated.

2.10 Invasion assay

Tumour cells were labelled with CM-Dil and serum starved for 24 hours. The labelled cells were cultured alone, treated with 50 ng/ml cytokines or mixed with MSCs in the upper part of Matrigel coated Boyden chambers (8 μM, BD Biosciences, San Jose, CA, USA). Cell invasion was determined by analysing the number of labelled cells that migrated through the Matrigel. The effect of CCL2 or IL6 was determined by adding 2 μg/ml anti-CCL2 antibody, 10 μg/ml anti-IL6 antibody or 4 μg/ml IL1RA to the tumour cell/MSC mixtures. The control was mouse IgG2b.

2.11 Differentiation of promyelocytic cells to macrophage-like cells

HL60 cells were plated at a density of $4x10^5$ cells/ml and differentiated with 12-O-tetradecanoylphorbol-13-acetate (TPA) (Sigma, Darmstadt, Germany) at a final concentration of 32 nM for six days. For the determination of CCL2, differentiated and undifferentiated cells were added to MSCs treated with conditioned medium from PancTu1 cells for 48 hours.

2.12 TCGA expression analysis

Expression data from the pancreatic cancer patient cohort were downloaded from The Cancer Genome Atlas (TCGA) Research Network (https://cancergenome.nih.gov/). RNaseq V2 level 3 data were downloaded for 186 pancreatic cancer samples from the TCGA data portal. The z-score threshold was set at 1.5. The downloaded dataset was parsed and visualized in R. The heatmaps were plotted using the R package ComplexHeatmap [58]. The script used is available at https://github.com/chrisclarkson/FASLG_heatmap_analysis.

3. Results

3.1 Tumour-bearing animals show an increase in MSC numbers

In order to study the fate of murine (mMSCs) and human (hMSCs) MSCs in tumour-bearing animals, we initially used the MDA-MB-231 mammary carcinoma model, for which MSC-promoted metastasis development had been previously described [42, 43]. To analyse MSC biodistribution, we intravenously injected CM-Dil labelled MSCs when the MDA-MB-231 xenografts became palpable (Figure 1A). For both mMSCs (Figure 1B and Supplementary Figure 1A) and hMSCs (Figure 1C and Supplementary Figure 1B), we found an increase in MSC numbers in the tumour-bearing animals, as compared to those carrying no xenograft. This increase only became visible four-weeks post-injection, whereas it was not apparent after one week, demonstrating that tumour-induced MSC proliferation is the cause of the observed effect.

For the purpose of studying the impact of this effect on tumour progression, in addition to MDA-MB-231 cells, we used the PancTu1 pancreatic cancer model (Figure 1A). While MDA-MB-231 cells show a degree of metastasis without MSCs, PancTu1 cells do not show metastasis when grown as subcutaneous xenograft [59]. Therefore, we first examined whether MSCs were able to induce metastasis development in the PancTu1 model. Four weeks after the injection of mMSCs, we evaluated H&E stained sections from the lungs of animals with MDA-MB-231 and PancTu1 xenografts for evidence of metastasis. In the cohorts that received MSCs, we found that more than half of the mice had developed metastatic lesions in the MDA-MB-231 model, while 83% of the mice with PancTu1-derived xenografts developed metastatic lesions (Figure 1D). On the contrary, in animals which did not receive MSCs, we could detect lung metastatic nodules in only 14% for

MDA-MB-231 tumours, and as expected, none for PancTu1 xenografts (Figure 1D). These results demonstrate that MSCs can exert their pro-metastatic function onto cells which normally do not disseminate. PancTu, therefore, represent a cleaner and better model to study the effect of tumour-induced MSC proliferation on metastasis development.

3.2 FasL induces proliferation in MSCs via MAPK/ERK

Increased FasL expression has been detected in various cancer types, including breast and pancreatic cancer [17, 20-23]. This can provide the proliferative signal for circulating MSCs and/or MSCs in the TME. However, FasL is a member of the TNF superfamily (TNFSF), and a so-called death ligand which is normally associated with apoptosis induction. In order to reconcile the pro-apoptotic function with a role in MSC proliferation and consequent tumour progression, MSCs would have to be resistant to FasL-induced apoptosis. To test whether MSCs are principally able to respond to FasL, we measured the levels of its receptor (Fas) on the surface of different types of hMSCs and mMSCs. While we found robust Fas expression for all MSC types, demonstrating that they should be able to respond (Figure 2A), all of them were resistant to up to 5 ng/ml of FasL (Figure 2B). Treatment with agonistic Fas antibodies also failed to trigger cell death in MSCs (Supplementary Figure 2A). Apoptosis was only detectable in both hMSCs and mMSCs when potent multimeric-FasL was used at high concentrations (5 ng/ml) (Supplementary Figure 2A). The multimeric-FasL led to Caspase-8 and -3 processing (Supplementary Figure 2B), and the induced cell death could be inhibited by the pan-caspase inhibitor zVAD (Supplementary Figure 2C). These findings indicate that MSCs have the potential

to trigger programmed cell death, but that Fas is configured to respond very weakly to its ligand with respect to apoptosis-induction.

In comparison to the effect of high concentrations of multimeric-FasL, treatment of different types of human and murine MSCs with low levels of FasL (0.2 ng/ml) gave rise to increased proliferation over a period of five days (Figure 2C). Similar results were also achieved in an outgrowth assay (Supplementary Figure 2D). At higher concentrations of FasL, the proliferative activity was lost, and MSCs did not grow more than the controls over the five-day period (Figure 2D). In addition, we examined whether agonistic Fas antibodies could also induce proliferation in MSCs. In contrast to FasL and multimeric-FasL, treatment with these antibodies did not give rise to enhanced proliferation in MSCs (Supplementary Figure 2E). As FasL acts as a trimer, engaging trimeric Fas receptor complexes compared to agonistic antibodies that tend to lead to dimeric forms, we concluded that receptor trimers are required for Fas signalling and proliferation of MSCs. Contrary to the FasL findings, TRAIL, another apoptosis-inducing member of the TNFSF, did not promote MSC proliferation (Supplementary Figure 2F).

Next, we analysed a number of non-apoptotic pathways which can be triggered by Fas signalling. Treatment of MSCs with 0.2 ng/ml FasL, and subsequent western blotting of the resulting protein lysates, showed that MAPK/ERK was substantially phosphorylated/activated, whereas JNK and p38 only showed a very transient peak in phosphorylation/activation (Figure 2E). The use of inhibitors revealed that blocking JNK or p38 had no impact on FasL-induced MSC proliferation (Figure 2F). In contrast, MAPK/ERK inhibitors reduced proliferation back to normal control levels (Figure 2F). Thus, FasL acts via MAPK/ERK to induce MSC proliferation.

3.3 Pancreatic cancer cells stimulate MSCs to produce the pro-metastatic cytokines CCL2 and IL6

The chemokine CCL5 and its receptor CCR5 have been implicated in MSC-mediated breast cancer metastasis [43]. Breast cancer cells were shown to stimulate secretion of CCL5 from MSCs, which then acts in a paracrine fashion on the cancer cells to enhance motility, invasion and metastasis. Therefore, we initially examined whether FasL could directly induce CCL5 expression in MSCs, while simultaneously instigating proliferation. When FasL (or multimeric-FasL; or agonistic Fas antibodies) was added to human or murine MSCs, there was no detectable change in CCL5 levels by ELISA (Figure 3A). Next, we tested whether crosstalk with pancreatic cancer cells induced CCL5 in MSCs, similar to MDA-MB-231 breast cancer cells. Indeed, when MDA-MB-231 cells were mixed with increasing numbers of mMSC, a substantial increase in CCL5 production and secretion, in an MSC-dose dependent manner, was evident (Figure 3B). However, when PancTu1 pancreatic cancer cells were used in such mixing experiments, CCL5 induction was not detected, irrespective of the number of MSCs (Figure 3B). The same pattern of CCL5 production was seen with hMSCs, where MDA-MB-231 cells led to the induction of CCL5 while PancTu1 cells did not (Figure 3C). Testing three additional pancreatic cancer cell lines (MiaPaCa2, AsPC1 and BxPC3) resulted in the same outcome (Figure 3D). Thus, it is evident that CCL5 cannot explain the MSC-induced metastasis development in our pancreatic cancer model (Figure 1D).

To identify potential factors involved in the MSC-induced metastatic phenotype, PancTu1 cells and hMSC supernatants (with and without co-culture) were screened using a cyto-/chemokine array for factors that were induced by the interaction of the two cell types.

CCL2 was found to be upregulated and secreted into the supernatant medium (Figure 3E). In addition, a significant increase in IL6 production was also evident, albeit starting from a higher basal level. Other factors on the array, such as IL8, GRO chemokines (CXCL1, CXCL2 and CXCL3) and several others, were not affected (Figure 3F). The induction of CCL2 and IL6 were corroborated by ELISA, which showed elevated levels of the two cytokines with increasing MSC numbers, i.e. mixing more hMSCs with a constant number of PancTu1 cells led to more cytokine production (Figure 3G). Moreover, mMSCs responded in the same way to mixing them with PancTu1 cells (Figure 3H). These results point to MSCs as a specific cellular production site for CCL2 and IL6 in response to interaction with pancreatic cancer cells. This hypothesis was confirmed using a murine CCL2-ELISA of supernatants of PancTu1/mMSCs and PancTu1/hMSCs mixes, of which only the former provided a positive result (Figure 3H). When we used cells from other cancer types (breast, colorectal and prostate cancer) and mixed them with hMSCs, we could not detect CCL2 and IL6 production (Figure 3I) indicating a specific effect in pancreatic cancer.

3.4 A pancreatic cancer cell-derived soluble factor is responsible for the induction of CCL2 and IL6 in MSCs

Pro-metastatic functions have been attributed to CCL2 and IL6 in various cancer types. Therefore, the direct action of recombinant CCL2 and IL6 on pancreatic cancer cells was analysed. In Matrigel assays, recombinant CCL2 was found to increase the invasiveness of PancTu1 cells, whereas IL6 only showed a moderate and non-significant effect (Figure 4A). Using PancTu1/MSC mixes, along with neutralising CCL2 or IL6 antibodies, it was

revealed that the blockage of CCL2 significantly reduced the invasiveness of PancTu1 cells (Figure 4B). These results demonstrate that pancreatic cancer cells can directly respond to MSC-produced CCL2.

In order to understand the mechanisms behind the up-regulation of CCL2 and IL6 in MSCs, we investigated whether cell-to-cell interactions are necessary to induce these cytokines. Transferring conditioned medium from PancTu1 cells onto hMSCs revealed increased levels of CCL2 and IL6 after 48 hours (Figure 4C). The same results were obtained with mMSCs (Supplementary Figure 3A). These results again confirm the notion that MSCs produce the two cytokines and show that a soluble factor secreted by the pancreatic cancer cells is responsible for the CCL2 and IL6 induction. This induction was not triggered by FasL produced by PancTu1 cells, as supplementing the supernatant with FasL-neutralising antibody did not inhibit the production of CCL2 and IL6 by hMSCs (Supplementary Figure 3B). Furthermore, 0.2 ng/ml FasL could not induce CCL2 and IL6 in hMSCs (Supplementary Figure 3B). Thus, another pancreatic cancer cell-derived factor has to be responsible for the cytokine induction.

Interestingly, hMSCs express relatively high basal levels of IL6 (Figure 3E), which is known to be able to stimulate CCL2 as well as its own expression [60]. Therefore, it was hypothesised that IL-6R trans-signalling [61], in which constitutive IL6, secreted by MSCs acting in concert with cancer cell-derived sIL6R, causes the production of CCL2 and additional IL6. Examining the supernatant of PancTu1 cells indeed revealed that they produce sIL6R, albeit at low levels (Figure 4D). In addition, treatment of hMSCs with recombinant sIL6R enhanced CCL2 production (Figure 4E). However, the addition of IL6 neutralising antibodies with the PancTu1 supernatants did not reduce induction of CCL2

(Figure 4F). We observed the same outcome with a STAT3 inhibitor, confirming that IL6 (trans-) signalling was not responsible for the effects exerted by the pancreatic cancer cells (Figure 4G).

Since IL6 is not responsible for the observed CCL2 induction, longer exposure images of the cytokine arrays were examined. The focus was on the factors which were present in the supernatants of the cancer cells but lacking from the medium of MSCs, instead of focusing on the induced factors. A total of seven cytokines and growth factors, IGF1, IL1α, IL1β, OSM, PDGF-BB, TPO and VEGF-A were identified (Figure 4H). Of these, recombinant IL1α, IL1β , OSM and PDGF-BB were able to induce CCL2 expression in hMSCs (Figure 4I). As neither a PI3K inhibitor to block PDGF signaling nor recombinant gp130 to block OSM could inhibit CCL2 induction by PancTu1 medium supernatants, IL1 (IL1α and IL1β) was left as the remaining candidate (Figure 4J and 4K). A role for IL1α and IL1β was supported by the observation that they could also induce IL6 in human MSCs (Figure 4L) as well as CCL2 and IL6 in mMSCs (Figure 4M).

3.5 Pancreatic cancer-derived IL1 induces CCL2 and IL6 via NF-κB activation in MSCs

In order to confirm that PancTu1-derived IL1 induces CCL2 and IL6 in MSCs, recombinant IL1RA, a natural IL1 receptor antagonist, was added to the cells. Importantly, MSC-produced CCL2 as well as IL6 were significantly reduced following addition of the antagonist (Figure 5A). Moreover, IL1RA was also able to block CCL2 and IL6 induction in hMSCs by three additional pancreatic cell lines (Figure 5B), indicating a general role of pancreatic cancer cell-derived IL1. Additionally, ELISA analyses revealed that both IL1α and IL1β are produced by pancreatic cancer cells (Figure 5C). As IL1 is a strong inducer

of NF-κB, the question arose whether PancTu1 supernatants would give rise to NF-κB activation in MSCs. Indeed, IκBα was degraded in MSCs 5-30 minutes after exposure to PancTu1 supernatants, and NF-κB was induced six-fold (Figure 5D). The NF-κB activation could be blocked by adding IL1RA to the pancreatic cancer cell supernatants (Figure 5D). In addition, an NF-κB inhibitor could stop the induction of CCL2 and IL6 by PancTu1 supernatants (Figure 5E), demonstrating the existence of an IL1-NF-κB-CCL2/IL6 pathway in MSCs in response to pancreatic cancer cells.

Finally, to demonstrate that FasL-induced proliferation of MSCs directly leads to an increased production of CCL2 and IL6 in response to IL1, we treated hMSCs with 0.2 ng/ml FasL for three days, followed by IL1 for 48 hours. We were able to measure significantly higher levels of CCL2 and IL6 in the supernatants of FasL-treated MSCs as compared to untreated controls, which reflects the higher concentration of MSCs in the FasL-stimulated samples (Supplementary Figure 4).

3.6 IL1 gives rise to sustained CCL2 and IL6 production in MSCs and monocytic cells inhibit the induction of the two cytokines

Next, we analysed how sustained the CCL2 and IL6 production by MSCs was. For this we removed the supernatants from induced MSCs every three days and replaced it with fresh growth medium. At the end of the experiment, significantly elevated concentrations of CCL2 and IL6 were still detectable, albeit at lower levels compared to when they were left to accumulate over nine days without a medium change (Figure 6A). These results show that MSCs, once triggered, can persistently produce pro-metastatic cytokines, thereby achieving a potentially wide and long-lasting impact on surrounding cells.

Anti-cancer therapeutic strategies targeting CCL2 activities have so far been unsuccessful in clinical studies [62], which is contrary to robust anti-tumour responses in several pre-clinical cancer models [63-68]. We wondered whether our results could be linked to these problems, in particular, the clinical finding that blocking CCL2 only transiently reduced serum CCL2 levels before they started to gradually increase and finally exceeded pretreatment baseline values [69]. In this context, we found that macrophage-like monocytic cells express IL1RA (Figure 6B), and when we added such cells to the PancTu1 cells and MSCs mix, we could measure a significant reduction in CCL2 production (Figure 6C). Thus, CCL-2 recruited monocytic cells might form a negative feedback loop which may limit the production of CCL2 in MSCs, and treatment with anti-CCL2 antibodies might break this mechanism. Given these difficulties with CCL2-blocking approaches, we sought to investigate the Fas/FasL system in MSCs as a potential alternative target to block metastasis.

3.7 Fas-deficient MSCs do not promote metastasis development

To further examine the importance of Fas signalling in MSC-induced tumour progression, we used MSCs established from MRL/MpJ-Fas^{lpr} mice (LPR-MSCs). These mice carry a mutation in the *Fas* gene, and consequently, LPR-MSCs show substantially reduced Fas protein expression as assessed by western blot and undetectable Fas surface expression measured by flow cytometry (Figure 7A). Therefore, in contrast to normal MSCs, LPR-MSC growth was not induced by low-level FasL stimulation, demonstrating that they possess no functionally relevant expression of Fas (Figure 7B). Importantly, in animals bearing PancTu1 tumours, the total number of LPR-MSCs was lower when compared to

mice injected with regular mMSCs, suggesting that the lack of Fas prevented proliferation of LPR-MSCs *in vivo* (Figure 7C). When we evaluated these LPR-MSC-injected mice for metastatic lesions, we found none, as compared to three of four animals in a control cohort injected with normal mMSCs (Figure 7D). LPR-MSCs are, however, capable to induce CCL2 and IL6 to the same extent as regular mMSCs when combined with PancTu1 cells. Addition of a FasL-neutralising antibody did not, similarly to hMSCs, change the induction of the two cytokines in both mMSCs and LPR-MSCs (Supplementary Figure 5A). These results indicate that without the FasL/Fas induced proliferation, the static number of LPR-MSCs do not produce sufficient levels of pro-metastatic factors to induce metastasis. Thus, targeting Fas signalling in MSCs might be a strategy to prevent tumour cells from progressing and metastasising, and in addition, knocking-out Fas by gene editing might be an approach to make MSCs safer for cell therapeutic applications.

To explain the tumour-dependent and Fas-mediated MSC proliferation, we tested PancTu1 cells for FasL expression. However, neither an ELISA nor supernatant transfer onto FasL-sensitive Jurkat cells showed any indication for FasL being expressed by PancTu1 cells (Supplementary Figure 5B and 5C). To rule out membrane bound FasL, we mixed PancTu1 and Jurkat cells, but similar to the supernatant transfer experiments, we were unable to find an apoptosis induction in the Jurkat cells which might have indicated the presence of FasL (Supplementary Figure 5D). Moreover, mixing experiments of MSCs and PancTu1 cells did not show signs of FasL induction caused by the interaction of the two cell types (Supplementary Figure 5D). Hence, we found no evidence that the cancer cells (or MSCs) express FasL. Another cell type in tumour-bearing mice must be the source of FasL, such as endothelial or immune-effector cells.

Our results establish a network of cancer cells and MSCs responding to and acting via FasL, IL1, CCL2 and IL6. To evaluate whether this FasL-IL1-CCL2-IL6 circuit exists in pancreatic cancer patients, bioinformatic co-expression analysis was performed on RNA-sequencing (RNA-seq) data from a cohort of 186 pancreatic adenocarcinoma samples. This analysis revealed that FasL expression showed a remarkable and significant positive correlation with the expression of two MSC markers (NGFR and Endoglin), CCL2 and IL6 as well as monocyte specific markers (CCR2 and MRC1) (Figure 7E and Supplementary Figure 5E). Furthermore, high CCL2 expression was associated with increased levels of the monocytic markers CCR2 and MRC1 (Figure 7F and Supplementary Figure 5F). Finally, IL1β, but not IL1α, was co-expressed with CCL2, IL6, CCR2 and MRC1 (Figure 7G and Supplementary Figure 5G). In contrast to FasL, TRAIL (TNFSF10) expression was not correlated to the two MSC markers NGFR and Endoglin (Supplementary Figure 5H). These results demonstrate that in human pancreatic cancer, FasL appears to give rise to an increase in MSCs which, in response to IL1, prompt the production of CCL2 and IL6. These cytokines, aside from affecting the cancer cells directly, also appear to mediate the recruitment of monocytic cells (Figure 8).

4. Discussion

MSCs have been shown to promote tumour metastasis in various cancer models [42, 43, 70-72], however, not all underlying cellular and molecular mechanisms have been characterised. Here, we show that Fas signalling in MSCs is required for their pro-metastatic activity, as MSCs lacking functional Fas expression do not lead to tumour progression in a pancreatic cancer model. Mechanistically, MSCs were found to be resistant to FasL-induced apoptosis, and low concentrations of FasL triggered so-called Fas-threshold signalling, promoting proliferation. This response was absent in LPR-MSCs. In line with these *in vitro* data, fewer LPR-MSCs were found in tumour-burdened mice, compared to when mice were injected with regular MSCs. These results link FasL/Fas-mediated-proliferation of MSCs to their capacity to promote metastasis development. While tumour-promoting activities of Fas and its ligand FasL have been reported before [33], our findings expand this role to MSCs in the TME.

There are several different possible sources of FasL in the context of a growing tumour. One possibility is that tumour-associated endothelial cells express FasL on their surface, providing the proliferation signal to MSCs when they infiltrate the tumour tissue [32, 73, 74]. Other reports have indicated that (pancreatic) cancer cells themselves express FasL [75], but we were unable to confirm these findings. Regardless of the origin of FasL, we found that in human pancreatic cancer, enhanced FasL expression is associated with higher levels of MSC-markers in the tumour. The FasL-induced increase in MSCs consequently provides a greater capacity to produce pro-metastatic factors.

In a breast carcinoma model, CCL5 was identified as the pro-metastatic cytokine which causes MSC-induced metastasis development [43]. However, we were unable to find

elevated CCL5 when MSCs were combined with pancreatic cancer cells. Instead, we discovered CCL2 and IL6 to be induced after interaction of pancreatic cancer cells with MSCs, identifying MSCs as a novel cellular production site for CCL2 and IL6 in the TME. Importantly, this induction gave rise to prolonged expression of the two cytokines, providing a longer window of action in which they can exert their pro-metastatic activities. Furthermore, we discovered that pancreatic cancer cell-derived IL1 is responsible for the CCL2 and IL6 induction via NF-κB activation in MSCs, as both an NF-κB inhibitor and the natural antagonist of the IL1 receptor, IL1RA, could fully inhibit the CCL2 and IL6 induction.

The two cytokines, CCL2 and IL6, possess well documented pro-metastatic activities [62, 76]. IL6 is a pleiotropic cytokine known to be involved in chronic inflammation and auto-immune diseases, but has also been shown to contribute to the generation of a pro-tumorigenic microenvironment, regulating angiogenesis and metastasis [77-80]. In the serum of pancreatic cancer patients, IL6 was found at elevated levels, which correlates with advanced tumour stage and poor survival [81]. Furthermore, knocking-out IL6 in a transgenic mouse model of pancreatic cancer inhibited the maintenance and progression of pancreatic cancer precursor lesions [82]. As we were unable to measure a direct impact of IL6 on the invasiveness of pancreatic cancer cells, it is likely that IL6 exerts its pro-metastatic effect via indirect mechanisms engaging additional cell types [79].

CCL2 is a small chemokine which belongs to the CC chemokine family [83]. Although first described as a chemotactic molecule for monocytes, basophils, T-lymphocytes and NK cells with physiological roles in regulating inflammation, more recent studies have revealed a pro-tumorigenic function for CCL2 favouring cancer development and

subsequent metastasis [84, 85]. Indeed, cancer progression and poor prognosis have been linked to enhanced levels of CCL2 in a number of cancer types, including pancreatic cancer [68, 86-89]. Therefore, CCL2 was proposed as a therapeutic target, which led to several clinical trials with anti-CCL2 antibodies in solid and metastatic cancers [62]. However, it became clear in these studies that CCL2 could only be transiently suppressed, and the CCL2 concentration gradually increased to levels beyond pre-treatment baseline values. Moreover, none of the treated patients showed an objective anti-tumour response [69, 90, 91].

It is known that CCL2 can exert direct actions on cancer cells as demonstrated in this study, as well as initiate the infiltration of pro-metastatic cell types including monocytes [67, 92]. We hypothesised that monocytic cells might also be involved in the regulation of CCL2 expression in MSCs, as we and others have shown that they express IL1RA [93, 94]. Indeed, when we combined monocytic cells with MSCs and conditioned medium from pancreatic cancer cells, CCL2 production was no longer induced. These findings provide a possible explanation for the rebounding CCL2 levels observed in clinical tests of anti-CCL2 antibodies. Despite failing in clinical tests, the anti-CCL2 antibodies afforded an initial reduction in the number of monocytic cells in the tumours. However, as monocytic cells normally carry IL1RA to tumours, they can limit the production of CCL2. While blocking CCL2 will give rise to a reduction in monocytic cells in the tumour, it will also lead to continuous and unchecked CCL2 production by MSCs. The loss of this homeostatic feedback mechanism can eventually overwhelm the capacity of the neutralising antibodies, leading to an overshoot of the CCL2 levels as observed in clinical studies. Therefore, targeting factors, such as FasL or IL1, which act on MSCs, might offer better alternatives.

Overall, our results establish MSCs as a central cellular player in the TME of pancreatic cancer, orchestrating a range of molecular and cellular changes that contribute to tumour progression and metastasis development.

Acknowledgments

We thank Stella-Maris Albarenque and Jamie Moore for their assistance with this project. This work was supported by an EU-FP6 Marie-Curie Excellence Team Award (MIST). The work was also supported by an EU-RTN Award (ApopTrain) and a Research Frontier Project Grant from Science Foundation Ireland (BIM084).

Author contribution

AM, VBT, GNB and RMZ supervised the study; AM performed animal experiments and in vitro experiments, and analysed data; TC and GNB completed and analysed *in vitro* studies; CTC analysed patient data and generated heatmaps; AM and RMZ wrote the paper; VBT, GNB and CTC edited the manuscript.

Conflict of Interest

The authors indicate no potential conflicts of interest.

References

[1] M.R. Rippo, L. Babini, F. Prattichizzo, L. Graciotti, G. Fulgenzi, F. Tomassoni Ardori, F. Olivieri, G. Borghetti, S. Cinti, A. Poloni, F. Fazioli, A.D. Procopio, Low FasL levels promote proliferation of human bone marrow-derived mesenchymal stem cells, higher levels inhibit their differentiation into adipocytes, Cell Death Dis., 4 (2013) e594.
[2] M. Studeny, F.C. Marini, R.E. Champlin, C. Zompetta, I.J. Fidler, M. Andreeff, Bone marrow-derived mesenchymal stem cells as vehicles for interferon-beta delivery into tumors, Cancer Res., 62 (2002) 3603-3608.
[3] C. Scaffidi, S. Fulda, A. Srinivasan, C. Friesen, F. Li, K.J. Tomaselli, K.M. Debatin, P.H. Krammer, M.E. Peter, Two CD95 (APO-1/Fas) signaling pathways, EMBO J., 17 (1998) 1675-1687.
[4] C. Scaffidi, I. Schmitz, J. Zha, S.J. Korsmeyer, P.H. Krammer, M.E. Peter, Differential modulation of apoptosis sensitivity in CD95 type I and type II cells, J. Biol. Chem., 274 (1999) 22532-22538.
[5] A.M. Kober, S. Legewie, C. Pforr, N. Fricker, R. Eils, P.H. Krammer, I.N. Lavrik, Caspase-8 activity has an essential role in CD95/Fas-mediated MAPK activation, Cell Death Dis., 2 (2011) e212.
[6] S.M. Lee, E.J. Kim, K. Suk, W.H. Lee, Stimulation of Fas (CD95) induces production of pro-inflammatory mediators through ERK/JNK-dependent activation of NF-kappaB in THP-1 cells, Cell. Immunol., 271 (2011) 157-162.
[7] P. Legembre, B.C. Barnhart, M.E. Peter, The relevance of NF-kappaB for CD95 signaling in tumor cells, Cell Cycle, 3 (2004) 1235-1239.
[8] C. Roder, A. Trauzold, H. Kalthoff, Impact of death receptor signaling on the malignancy of pancreatic ductal adenocarcinoma, Eur. J. Cell Biol., 90 (2011) 450-455.
[9] D. Siegmund, S. Klose, D. Zhou, B. Baumann, C. Roder, H. Kalthoff, H. Wajant, A. Trauzold, Role of caspases in CD95L- and TRAIL-induced non-apoptotic signalling in pancreatic tumour cells, Cell. Signal., 19 (2007) 1172-1184.
[10] H. Wajant, K. Pfizenmaier, P. Scheurich, Non-apoptotic Fas signaling, Cytokine Growth Factor Rev., 14 (2003) 53-66.
[11] M. Bentele, I. Lavrik, M. Ulrich, S. Stosser, D.W. Heermann, H. Kalthoff, P.H. Krammer, R. Eils, Mathematical modeling reveals threshold mechanism in CD95-induced apoptosis, J. Cell Biol., 166 (2004) 839-851.
[12] I.N. Lavrik, A. Golks, D. Riess, M. Bentele, R. Eils, P.H. Krammer, Analysis of CD95 threshold signaling: triggering of CD95 (FAS/APO-1) at low concentrations primarily results in survival signaling, J. Biol. Chem., 282 (2007) 13664-13671.
[13] M. Paulsen, S. Valentin, B. Mathew, S. Adam-Klages, U. Bertsch, I. Lavrik, P.H. Krammer, D. Kabelitz, O. Janssen, Modulation of CD4+ T-cell activation by CD95 co-stimulation, Cell Death Differ., 18 (2011) 619-631.
[14] P. Legembre, B.C. Barnhart, L. Zheng, S. Vijayan, S.E. Straus, J. Puck, J.K. Dale, M. Lenardo, M.E. Peter, Induction of apoptosis and activation of NF-kappaB by CD95 require different signalling thresholds, EMBO Rep., 5 (2004) 1084-1089.
[15] E.J. Belt, H.B. Stockmann, P.M. Delis-van Diemen, H. Bril, M. Tijssen, H.F. van Essen, M.W. Heymans, J.A. Belien, B. Carvalho, S.A. Cillessen, G.A. Meijer, Expression of apoptosis regulating proteins identifies stage II and III colon cancer patients with high risk of recurrence, J. Surg. Oncol., 109 (2014) 255-265.

[16] C. Botti, S. Buglioni, M. Benevolo, D. Giannarelli, P. Papaldo, F. Cognetti, P. Vici, F. Di Filippo, F. Del Nonno, F.M. Venanzi, P.G. Natali, M. Mottolese, Altered expression of FAS system is related to adverse clinical outcome in stage I-II breast cancer patients treated with adjuvant anthracycline-based chemotherapy, Clin. Cancer Res., 10 (2004) 1360-1365.
[17] A.I. El-Sarha, G.M. Magour, S.M. Zaki, M.Y. El-Sammak, Serum sFas and tumor tissue FasL negatively correlated with survival in Egyptian patients suffering from breast ductal carcinoma, Pathol. Oncol. Res., 15 (2009) 241-250.
[18] C. Herrnring, T. Reimer, U. Jeschke, J. Makovitzky, K. Kruger, B. Gerber, D. Kabelitz, K. Friese, Expression of the apoptosis-inducing ligands FasL and TRAIL in malignant and benign human breast tumors, Histochem. Cell Biol., 113 (2000) 189-194.
[19] M. Mottolese, E.A. Nadasi, C. Botti, A.M. Cianciulli, R. Merola, S. Buglioni, M. Benevolo, D. Giannarelli, F. Marandino, R.P. Donnorso, I. Venturo, P.G. Natali, Phenotypic changes of p53, HER2, and FAS system in multiple normal tissues surrounding breast cancer, J. Cell. Physiol., 204 (2005) 106-112.
[20] L. Mullauer, I. Mosberger, M. Grusch, M. Rudas, A. Chott, Fas ligand is expressed in normal breast epithelial cells and is frequently up-regulated in breast cancer, J. Pathol., 190 (2000) 20-30.
[21] M. Muschen, C. Moers, U. Warskulat, D. Niederacher, B. Betz, J. Even, A. Lim, R. Josien, M.W. Beckmann, D. Haussinger, CD95 ligand expression in dedifferentiated breast cancer, J. Pathol., 189 (1999) 378-386.
[22] T. Ohta, A. Elnemr, H. Kitagawa, M. Kayahara, H. Takamura, T. Fujimura, G. Nishimura, K. Shimizu, S.Q. Yi, K. Miwa, Fas ligand expression in human pancreatic cancer, Oncol. Rep., 12 (2004) 749-754.
[23] N.L. Pernick, F.H. Sarkar, P. Tabaczka, G. Kotcher, J. Frank, N.V. Adsay, Fas and Fas ligand expression in pancreatic adenocarcinoma, Pancreas, 25 (2002) e36-41.
[24] J. Sjostrom, C. Blomqvist, K. von Boguslawski, N.O. Bengtsson, I. Mjaaland, P. Malmstrom, B. Ostenstadt, E. Wist, V. Valvere, S. Takayama, J.C. Reed, E. Saksela, The predictive value of bcl-2, bax, bcl-xL, bag-1, fas, and fasL for chemotherapy response in advanced breast cancer, Clin. Cancer Res., 8 (2002) 811-816.
[25] E. Song, J. Chen, N. Ouyang, F. Su, M. Wang, U. Heemann, Soluble Fas ligand released by colon adenocarcinoma cells induces host lymphocyte apoptosis: an active mode of immune evasion in colon cancer, Br. J. Cancer, 85 (2001) 1047-1054.
[26] W. Zhang, E.X. Ding, Q. Wang, D.Q. Zhu, J. He, Y.L. Li, Y.H. Wang, Fas ligand expression in colon cancer: a possible mechanism of tumor immune privilege, World J. Gastroenterol., 11 (2005) 3632-3635.
[27] B.C. Barnhart, P. Legembre, E. Pietras, C. Bubici, G. Franzoso, M.E. Peter, CD95 ligand induces motility and invasiveness of apoptosis-resistant tumor cells, EMBO J., 23 (2004) 3175-3185.
[28] L. Chen, S.M. Park, A.V. Tumanov, A. Hau, K. Sawada, C. Feig, J.R. Turner, Y.X. Fu, I.L. Romero, E. Lengyel, M.E. Peter, CD95 promotes tumour growth, Nature, 465 (2010) 492-496.
[29] F.J. Hoogwater, M.W. Nijkamp, N. Smakman, E.J. Steller, B.L. Emmink, B.F. Westendorp, D.A. Raats, M.R. Sprick, U. Schaefer, W.J. Van Houdt, M.T. De Bruijn, R.C. Schackmann, P.W. Derksen, J.P. Medema, H. Walczak, I.H. Borel Rinkes, O.

Kranenburg, Oncogenic K-Ras turns death receptors into metastasis-promoting receptors in human and mouse colorectal cancer cells, Gastroenterology, 138 (2010) 2357-2367.
[30] S. Kleber, I. Sancho-Martinez, B. Wiestler, A. Beisel, C. Gieffers, O. Hill, M. Thiemann, W. Mueller, J. Sykora, A. Kuhn, N. Schreglmann, E. Letellier, C. Zuliani, S. Klussmann, M. Teodorczyk, H.J. Grone, T.M. Ganten, H. Sultmann, J. Tuttenberg, A. von Deimling, A. Regnier-Vigouroux, C. Herold-Mende, A. Martin-Villalba, Yes and PI3K bind CD95 to signal invasion of glioblastoma, Cancer Cell, 13 (2008) 235-248.
[31] H.C. Lin, P.Y. Lai, Y.P. Lin, J.Y. Huang, B.C. Yang, Fas ligand enhances malignant behavior of tumor cells through interaction with Met, hepatocyte growth factor receptor, in lipid rafts, J. Biol. Chem., 287 (2012) 20664-20673.
[32] M. Malleter, S. Tauzin, A. Bessede, R. Castellano, A. Goubard, F. Godey, J. Leveque, P. Jezequel, L. Campion, M. Campone, T. Ducret, G. MacGrogan, L. Debure, Y. Collette, P. Vacher, P. Legembre, CD95L cell surface cleavage triggers a prometastatic signaling pathway in triple-negative breast cancer, Cancer Res., 73 (2013) 6711-6721.
[33] M.E. Peter, A. Hadji, A.E. Murmann, S. Brockway, W. Putzbach, A. Pattanayak, P. Ceppi, The role of CD95 and CD95 ligand in cancer, Cell Death Differ., 22 (2015) 549-559.
[34] M. Teodorczyk, S. Kleber, D. Wollny, J.P. Sefrin, B. Aykut, A. Mateos, P. Herhaus, I. Sancho-Martinez, O. Hill, C. Gieffers, J. Sykora, W. Weichert, C. Eisen, A. Trumpp, M.R. Sprick, F. Bergmann, T. Welsch, A. Martin-Villalba, CD95 promotes metastatic spread via Sck in pancreatic ductal adenocarcinoma, Cell Death Differ., 22 (2015) 1192-1202.
[35] A. Trauzold, C. Roder, B. Sipos, K. Karsten, A. Arlt, P. Jiang, J.I. Martin-Subero, D. Siegmund, S. Muerkoster, L. Pagerols-Raluy, R. Siebert, H. Wajant, H. Kalthoff, CD95 and TRAF2 promote invasiveness of pancreatic cancer cells, FASEB J., 19 (2005) 620-622.
[36] Y. Zhang, Q. Liu, M. Zhang, Y. Yu, X. Liu, X. Cao, Fas signal promotes lung cancer growth by recruiting myeloid-derived suppressor cells via cancer cell-derived PGE2, J. Immunol., 182 (2009) 3801-3808.
[37] H.X. Zheng, Y.D. Cai, Y.D. Wang, X.B. Cui, T.T. Xie, W.J. Li, L. Peng, Y. Zhang, Z.Q. Wang, J. Wang, B. Jiang, Fas signaling promotes motility and metastasis through epithelial-mesenchymal transition in gastrointestinal cancer, Oncogene, 32 (2013) 1183-1192.
[38] Y. Shi, L. Du, L. Lin, Y. Wang, Tumour-associated mesenchymal stem/stromal cells: emerging therapeutic targets, Nat. Rev. Drug Discov., 16 (2017) 35-52.
[39] F.R. Balkwill, M. Capasso, T. Hagemann, The tumor microenvironment at a glance, J. Cell Sci., 125 (2012) 5591-5596.
[40] A. Mohr, R. Zwacka, The future of mesenchymal stem cell-based therapeutic approaches for cancer - From cells to ghosts, Cancer Lett., 414 (2018) 239-249.
[41] M.F. Pittenger, A.M. Mackay, S.C. Beck, R.K. Jaiswal, R. Douglas, J.D. Mosca, M.A. Moorman, D.W. Simonetti, S. Craig, D.R. Marshak, Multilineage potential of adult human mesenchymal stem cells, Science, 284 (1999) 143-147.
[42] S.M. Albarenque, R.M. Zwacka, A. Mohr, Both human and mouse mesenchymal stem cells promote breast cancer metastasis, Stem Cell Res., 7 (2011) 163-171.

[43] A.E. Karnoub, A.B. Dash, A.P. Vo, A. Sullivan, M.W. Brooks, G.W. Bell, A.L. Richardson, K. Polyak, R. Tubo, R.A. Weinberg, Mesenchymal stem cells within tumour stroma promote breast cancer metastasis, Nature, 449 (2007) 557-563.
[44] Z. Mi, S.D. Bhattacharya, V.M. Kim, H. Guo, L.J. Talbot, P.C. Kuo, Osteopontin promotes CCL5-mesenchymal stromal cell-mediated breast cancer metastasis, Carcinogenesis, 32 (2011) 477-487.
[45] T.S. Chan, Y. Shaked, K.K. Tsai, Targeting the Interplay Between Cancer Fibroblasts, Mesenchymal Stem Cells, and Cancer Stem Cells in Desmoplastic Cancers, Front Oncol, 9 (2019) 688.
[46] T. Kamisawa, L.D. Wood, T. Itoi, K. Takaori, Pancreatic cancer, Lancet, 388 (2016) 73-85.
[47] Y. Sunami, V. Boker, J. Kleeff, Targeting and Reprograming Cancer-Associated Fibroblasts and the Tumor Microenvironment in Pancreatic Cancer, Cancers (Basel), 13 (2021).
[48] Y. Sunami, J. Haussler, J. Kleeff, Cellular Heterogeneity of Pancreatic Stellate Cells, Mesenchymal Stem Cells, and Cancer-Associated Fibroblasts in Pancreatic Cancer, Cancers (Basel), 12 (2020).
[49] B.M. Beckermann, G. Kallifatidis, A. Groth, D. Frommhold, A. Apel, J. Mattern, A.V. Salnikov, G. Moldenhauer, W. Wagner, A. Diehlmann, R. Saffrich, M. Schubert, A.D. Ho, N. Giese, M.W. Buchler, H. Friess, P. Buchler, I. Herr, VEGF expression by mesenchymal stem cells contributes to angiogenesis in pancreatic carcinoma, Br. J. Cancer, 99 (2008) 622-631.
[50] A. Kabashima-Niibe, H. Higuchi, H. Takaishi, Y. Masugi, Y. Matsuzaki, Y. Mabuchi, S. Funakoshi, M. Adachi, Y. Hamamoto, S. Kawachi, K. Aiura, Y. Kitagawa, M. Sakamoto, T. Hibi, Mesenchymal stem cells regulate epithelial-mesenchymal transition and tumor progression of pancreatic cancer cells, Cancer Sci., 104 (2013) 157-164.
[51] K. Saito, M. Sakaguchi, S. Maruyama, H. Iioka, E.W. Putranto, I.W. Sumardika, N. Tomonobu, T. Kawasaki, K. Homma, E. Kondo, Stromal mesenchymal stem cells facilitate pancreatic cancer progression by regulating specific secretory molecules through mutual cellular interaction, J Cancer, 9 (2018) 2916-2929.
[52] M. Waghray, M. Yalamanchili, M. Dziubinski, M. Zeinali, M. Erkkinen, H. Yang, K.A. Schradle, S. Urs, M. Pasca Di Magliano, T.H. Welling, P.L. Palmbos, E.V. Abel, V. Sahai, S. Nagrath, L. Wang, D.M. Simeone, GM-CSF Mediates Mesenchymal-Epithelial Cross-talk in Pancreatic Cancer, Cancer Discov, 6 (2016) 886-899.
[53] J. Drappa, N. Brot, K.B. Elkon, The Fas protein is expressed at high levels on CD4+CD8+ thymocytes and activated mature lymphocytes in normal mice but not in the lupus-prone strain, MRL lpr/lpr, Proc. Natl. Acad. Sci. U. S. A., 90 (1993) 10340-10344.
[54] R. Watanabe-Fukunaga, C.I. Brannan, N.G. Copeland, N.A. Jenkins, S. Nagata, Lymphoproliferation disorder in mice explained by defects in Fas antigen that mediates apoptosis, Nature, 356 (1992) 314-317.
[55] A. Mohr, T. Chu, G.N. Brooke, R.M. Zwacka, MSC.sTRAIL Has Better Efficacy than MSC.FL-TRAIL and in Combination with AKTi Blocks Pro-Metastatic Cytokine Production in Prostate Cancer Cells, Cancers (Basel), 11 (2019) 568.

[56] I. Nicoletti, G. Migliorati, M.C. Pagliacci, F. Grignani, C. Riccardi, A rapid and simple method for measuring thymocyte apoptosis by propidium iodide staining and flow cytometry, Journal of Immunological Methods 139 (1991) 271-279.
[57] A. Mohr, L. Deedigan, S. Jencz, Y. Mehrabadi, L. Houlden, S.M. Albarenque, R.M. Zwacka, Caspase-10: a molecular switch from cell-autonomous apoptosis to communal cell death in response to chemotherapeutic drug treatment, Cell Death Differ., 25 (2018) 340-352.
[58] Z. Gu, R. Eils, M. Schlesner, Complex heatmaps reveal patterns and correlations in multidimensional genomic data, Bioinformatics, 32 (2016) 2847-2849.
[59] F. Alves, S. Contag, M. Missbach, J. Kaspareit, K. Nebendahl, U. Borchers, B. Heidrich, R. Streich, W. Hiddemann, An orthotopic model of ductal adenocarcinoma of the pancreas in severe combined immunodeficient mice representing all steps of the metastatic cascade, Pancreas, 23 (2001) 227-235.
[60] S.M. Hurst, T.S. Wilkinson, R.M. McLoughlin, S. Jones, S. Horiuchi, N. Yamamoto, S. Rose-John, G.M. Fuller, N. Topley, S.A. Jones, Il-6 and its soluble receptor orchestrate a temporal switch in the pattern of leukocyte recruitment seen during acute inflammation, Immunity, 14 (2001) 705-714.
[61] F. Schaper, S. Rose-John, Interleukin-6: Biology, signaling and strategies of blockade, Cytokine Growth Factor Rev., 26 (2015) 475-487.
[62] S.Y. Lim, A.E. Yuzhalin, A.N. Gordon-Weeks, R.J. Muschel, Targeting the CCL2-CCR2 signaling axis in cancer metastasis, Oncotarget, 7 (2016) 28697-28710.
[63] K.Y. Teng, J. Han, X. Zhang, S.H. Hsu, S. He, N.A. Wani, J.M. Barajas, L.A. Snyder, W.L. Frankel, M.A. Caligiuri, S.T. Jacob, J. Yu, K. Ghoshal, Blocking the CCL2-CCR2 Axis Using CCL2-Neutralizing Antibody Is an Effective Therapy for Hepatocellular Cancer in a Mouse Model, Mol. Cancer Ther., 16 (2017) 312-322.
[64] E. Chun, S. Lavoie, M. Michaud, C.A. Gallini, J. Kim, G. Soucy, R. Odze, J.N. Glickman, W.S. Garrett, CCL2 Promotes Colorectal Carcinogenesis by Enhancing Polymorphonuclear Myeloid-Derived Suppressor Cell Population and Function, Cell reports, 12 (2015) 244-257.
[65] H. Fujimoto, T. Sangai, G. Ishii, A. Ikehara, T. Nagashima, M. Miyazaki, A. Ochiai, Stromal MCP-1 in mammary tumors induces tumor-associated macrophage infiltration and contributes to tumor progression, Int. J. Cancer, 125 (2009) 1276-1284.
[66] R.D. Loberg, C. Ying, M. Craig, L.L. Day, E. Sargent, C. Neeley, K. Wojno, L.A. Snyder, L. Yan, K.J. Pienta, Targeting CCL2 with systemic delivery of neutralizing antibodies induces prostate cancer tumor regression in vivo, Cancer Res., 67 (2007) 9417-9424.
[67] B.Z. Qian, J. Li, H. Zhang, T. Kitamura, J. Zhang, L.R. Campion, E.A. Kaiser, L.A. Snyder, J.W. Pollard, CCL2 recruits inflammatory monocytes to facilitate breast-tumour metastasis, Nature, 475 (2011) 222-225.
[68] D.E. Sanford, B.A. Belt, R.Z. Panni, A. Mayer, A.D. Deshpande, D. Carpenter, J.B. Mitchem, S.M. Plambeck-Suess, L.A. Worley, B.D. Goetz, A. Wang-Gillam, T.J. Eberlein, D.G. Denardo, S.P. Goedegebuure, D.C. Linehan, Inflammatory monocyte mobilization decreases patient survival in pancreatic cancer: a role for targeting the CCL2/CCR2 axis, Clin. Cancer Res., 19 (2013) 3404-3415.
[69] S.K. Sandhu, K. Papadopoulos, P.C. Fong, A. Patnaik, C. Messiou, D. Olmos, G. Wang, B.J. Tromp, T.A. Puchalski, F. Balkwill, B. Berns, S. Seetharam, J.S. de Bono,

A.W. Tolcher, A first-in-human, first-in-class, phase I study of carlumab (CNTO 888), a human monoclonal antibody against CC-chemokine ligand 2 in patients with solid tumors, Cancer Chemother. Pharmacol., 71 (2013) 1041-1050.
[70] Y. Jung, J.K. Kim, Y. Shiozawa, J. Wang, A. Mishra, J. Joseph, J.E. Berry, S. McGee, E. Lee, H. Sun, J. Wang, T. Jin, H. Zhang, J. Dai, P.H. Krebsbach, E.T. Keller, K.J. Pienta, R.S. Taichman, Recruitment of mesenchymal stem cells into prostate tumours promotes metastasis, Nat. Commun., 4 (2013) 1795.
[71] J. Luo, S. Ok Lee, L. Liang, C.K. Huang, L. Li, S. Wen, C. Chang, Infiltrating bone marrow mesenchymal stem cells increase prostate cancer stem cell population and metastatic ability via secreting cytokines to suppress androgen receptor signaling, Oncogene, 33 (2014) 2768-2778.
[72] W.T. Xu, Z.Y. Bian, Q.M. Fan, G. Li, T.T. Tang, Human mesenchymal stem cells (hMSCs) target osteosarcoma and promote its growth and pulmonary metastasis, Cancer Lett., 281 (2009) 32-41.
[73] M. Le Gallo, A. Poissonnier, P. Blanco, P. Legembre, CD95/Fas, Non-Apoptotic Signaling Pathways, and Kinases, Front Immunol, 8 (2017) 1216.
[74] G.T. Motz, S.P. Santoro, L.P. Wang, T. Garrabrant, R.R. Lastra, I.S. Hagemann, P. Lal, M.D. Feldman, F. Benencia, G. Coukos, Tumor endothelium FasL establishes a selective immune barrier promoting tolerance in tumors, Nat. Med., 20 (2014) 607-615.
[75] H. Ungefroren, M. Voss, M. Jansen, C. Roeder, D. Henne-Bruns, B. Kremer, H. Kalthoff, Human pancreatic adenocarcinomas express Fas and Fas ligand yet are resistant to Fas-mediated apoptosis, Cancer Res., 58 (1998) 1741-1749.
[76] T. Ara, Y.A. Declerck, Interleukin-6 in bone metastasis and cancer progression, Eur. J. Cancer, 46 (2010) 1223-1231.
[77] C. Garbers, S. Heink, T. Korn, S. Rose-John, Interleukin-6: designing specific therapeutics for a complex cytokine, Nat. Rev. Drug Discov., 17 (2018) 395-412.
[78] S. Kang, T. Tanaka, M. Narazaki, T. Kishimoto, Targeting Interleukin-6 Signaling in Clinic, Immunity, 50 (2019) 1007-1023.
[79] N. Kumari, B.S. Dwarakanath, A. Das, A.N. Bhatt, Role of interleukin-6 in cancer progression and therapeutic resistance, Tumour Biol., 37 (2016) 11553-11572.
[80] M. Murakami, D. Kamimura, T. Hirano, Pleiotropy and Specificity: Insights from the Interleukin 6 Family of Cytokines, Immunity, 50 (2019) 812-831.
[81] T. Miura, S. Mitsunaga, M. Ikeda, S. Shimizu, I. Ohno, H. Takahashi, J. Furuse, M. Inagaki, S. Higashi, H. Kato, K. Terao, A. Ochiai, Characterization of patients with advanced pancreatic cancer and high serum interleukin-6 levels, Pancreas, 44 (2015) 756-763.
[82] Y. Zhang, W. Yan, M.A. Collins, F. Bednar, S. Rakshit, B.R. Zetter, B.Z. Stanger, I. Chung, A.D. Rhim, M.P. di Magliano, Interleukin-6 is required for pancreatic cancer progression by promoting MAPK signaling activation and oxidative stress resistance, Cancer Res., 73 (2013) 6359-6374.
[83] J.W. Griffith, C.L. Sokol, A.D. Luster, Chemokines and chemokine receptors: positioning cells for host defense and immunity, Annu. Rev. Immunol., 32 (2014) 659-702.
[84] M.T. Chow, A.D. Luster, Chemokines in cancer, Cancer Immunol Res, 2 (2014) 1125-1131.

[85] T. O'Connor, L. Borsig, M. Heikenwalder, CCL2-CCR2 Signaling in Disease Pathogenesis, Endocr. Metab. Immune Disord. Drug Targets, 15 (2015) 105-118.
[86] C. Kudo-Saito, H. Shirako, M. Ohike, N. Tsukamoto, Y. Kawakami, CCL2 is critical for immunosuppression to promote cancer metastasis, Clin. Exp. Metastasis, 30 (2013) 393-405.
[87] X. Li, R. Loberg, J. Liao, C. Ying, L.A. Snyder, K.J. Pienta, L.K. McCauley, A destructive cascade mediated by CCL2 facilitates prostate cancer growth in bone, Cancer Res., 69 (2009) 1685-1692.
[88] Y. Lu, Z. Cai, D.L. Galson, G. Xiao, Y. Liu, D.E. George, M.F. Melhem, Z. Yao, J. Zhang, Monocyte chemotactic protein-1 (MCP-1) acts as a paracrine and autocrine factor for prostate cancer growth and invasion, Prostate, 66 (2006) 1311-1318.
[89] H. Yoshidome, H. Kohno, T. Shida, F. Kimura, H. Shimizu, M. Ohtsuka, Y. Nakatani, M. Miyazaki, Significance of monocyte chemoattractant protein-1 in angiogenesis and survival in colorectal liver metastases, Int. J. Oncol., 34 (2009) 923-930.
[90] K.J. Pienta, J.P. Machiels, D. Schrijvers, B. Alekseev, M. Shkolnik, S.J. Crabb, S. Li, S. Seetharam, T.A. Puchalski, C. Takimoto, Y. Elsayed, F. Dawkins, J.S. de Bono, Phase 2 study of carlumab (CNTO 888), a human monoclonal antibody against CC-chemokine ligand 2 (CCL2), in metastatic castration-resistant prostate cancer, Invest. New Drugs, 31 (2013) 760-768.
[91] M. Vela, M. Aris, M. Llorente, J.A. Garcia-Sanz, L. Kremer, Chemokine receptor-specific antibodies in cancer immunotherapy: achievements and challenges, Front Immunol, 6 (2015) 12.
[92] T. Hartwig, A. Montinaro, S. von Karstedt, A. Sevko, S. Surinova, A. Chakravarthy, L. Taraborrelli, P. Draber, E. Lafont, F. Arce Vargas, M.A. El-Bahrawy, S.A. Quezada, H. Walczak, The TRAIL-Induced Cancer Secretome Promotes a Tumor-Supportive Immune Microenvironment via CCR2, Mol. Cell, 65 (2017) 730-742 e735.
[93] W.P. Arend, F.G. Joslin, R.J. Massoni, Effects of immune complexes on production by human monocytes of interleukin 1 or an interleukin 1 inhibitor, J. Immunol., 134 (1985) 3868-3875.
[94] W.P. Arend, H.G. Welgus, R.C. Thompson, S.P. Eisenberg, Biological properties of recombinant human monocyte-derived interleukin 1 receptor antagonist, J. Clin. Invest., 85 (1990) 1694-1697.

Figures and Figure Legends

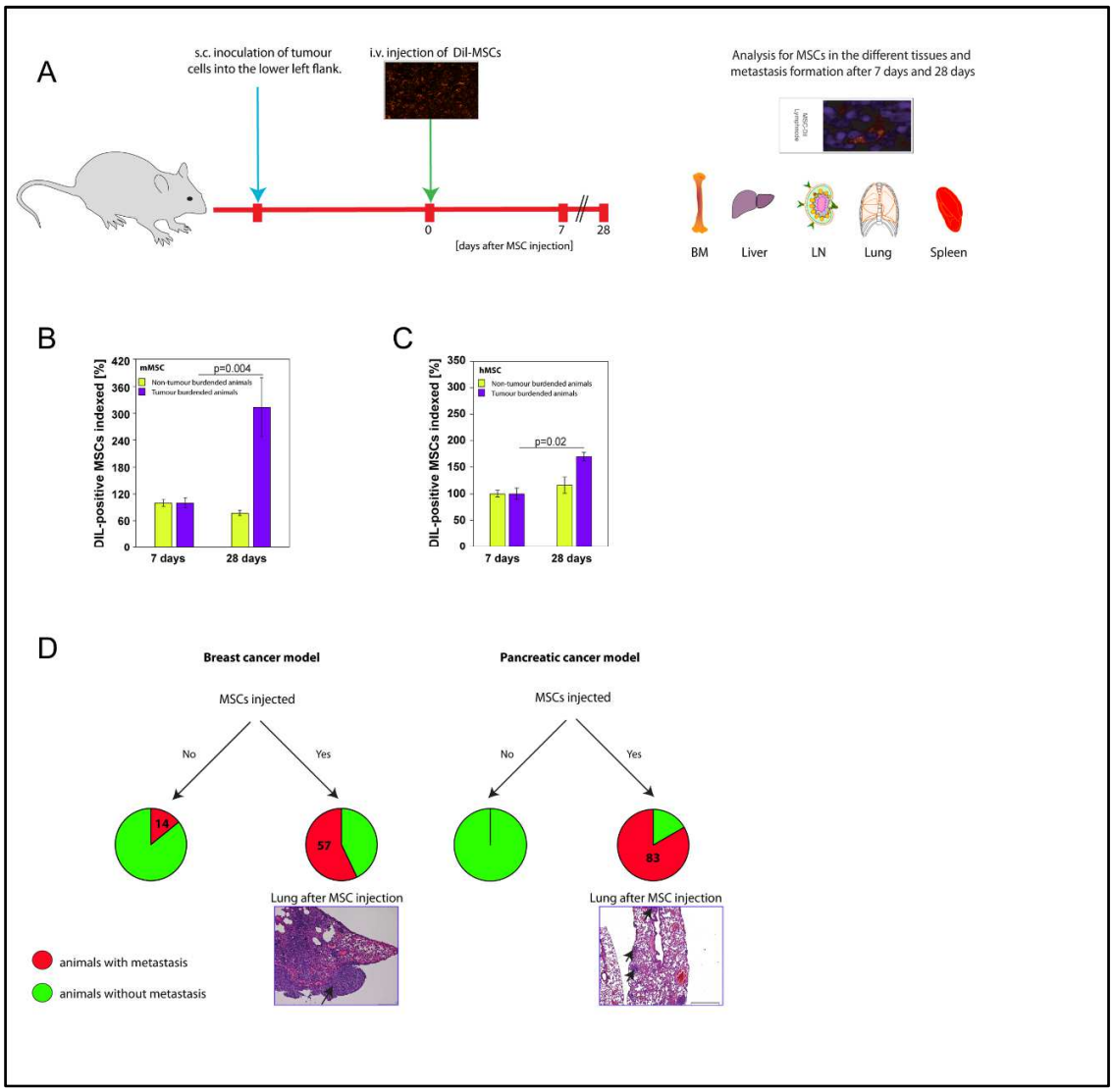

Figure 1. Tumour-burdened animals show an increase in MSC numbers.

(A) Schematic overview of experimental design to study MSC biodistribution, numbers and metastasis development.

(B, C) Relative numbers of murine MSCs (mMSCs) and human MSCs (hMSCs) found in control (yellow) and tumour-burdened (MDA-MB-231) animals (purple) after 7 days and 28 days, respectively. The relative numbers of MSCs found in the following tissues are shown in the diagram: bone marrow, lymph nodes, liver, lung and spleen. The average

numbers on day 7 were set to 100% to allow for comparison to the 28-day time point. Each cohort consisted of three animals.

(D) Incidence (%) of metastases in different tumour models (breast cancer, left; pancreatic cancer, right) after systemic murine MSC administration. Representative images of H/E stained lung microsection with metastatic lesions (black arrows) from tumour-burdened mice injected with MSCs are also shown. Each cohort consisted of six animals.

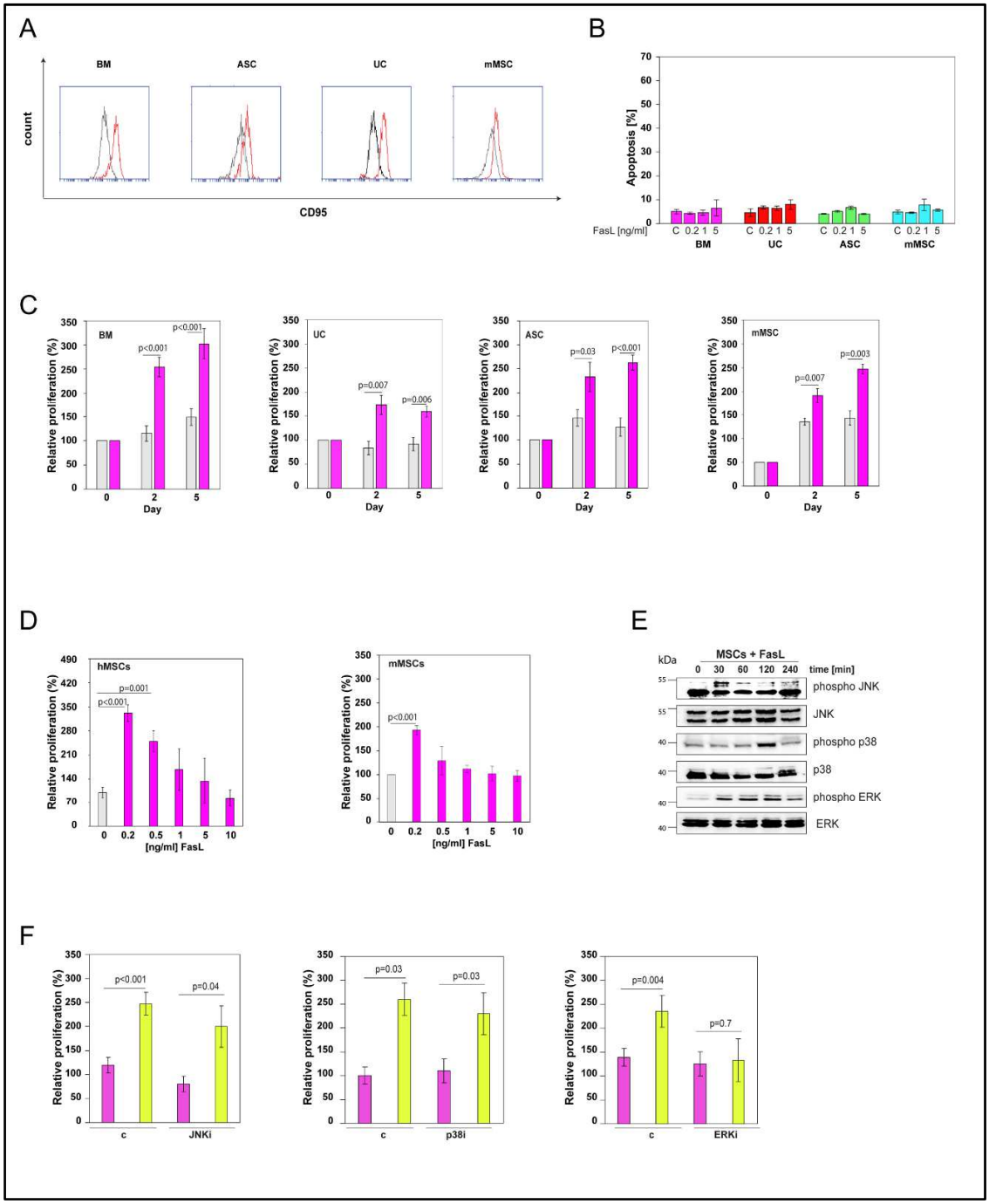

Figure 2. FasL induces proliferation in MSCs via MAPK/ERK.

(A) Representative histograms of flow cytometric analyses of Fas surface expression in human MSCs from bone marrow (BM), adipose tissue (ASC) and umbilical cord (UC) as well as murine MSCs (mMSC).

(B) Apoptosis measurements in different types of MSCs after treatment with recombinant FasL for 24 h, at concentrations ranging from 0.2-5 ng/ml. Controls (c) were treated with carrier only. Results are the mean ± SEM; n=3.

(C) Human MSCs from bone marrow (BM), umbilical cord (UC) and adipose tissue (ASC) as well as murine MSCs (mMSC) were treated with 0.2 ng/ml of FasL for 2 and 5 days and cell numbers determined (purple). MSCs treated with carrier are shown as controls (grey). The numbers of MSCs at the start of FasL treatment (Day 0) were set to 100%. Results are the mean ± SEM; (BM-MSCs ASC-MSCs n=8; UC-MSCs n=5; mMSCs n=6).

(D) Human (hMSC, left) and murine MSCs (mMSC, right) were treated with different concentrations of FasL, as shown in the figure, for 2 days. The numbers of MSCs at the start of FasL treatment (Day 0) were set to 100%. Results are the mean ± SEM; n=8.

(E) Murine MSCs were treated with 0.2 ng/ml FasL for 30, 60, 120 and 240 min and the resulting protein lysates analysed by western blot with phospho-specific antibodies against JNK, p38 and ERK. Western blots with regular antibodies served as loading controls.

(F) Murine MSCs were treated with 0.2 ng/ml FasL for 2 days, and JNKi (left), p38i (centre) and ERKi (right), respectively. The numbers of MSCs at the start of FasL treatment (Day 0) were set to 100%. Results are the mean ± SEM; n=4. Carrier treated controls (c) are shown as comparison.

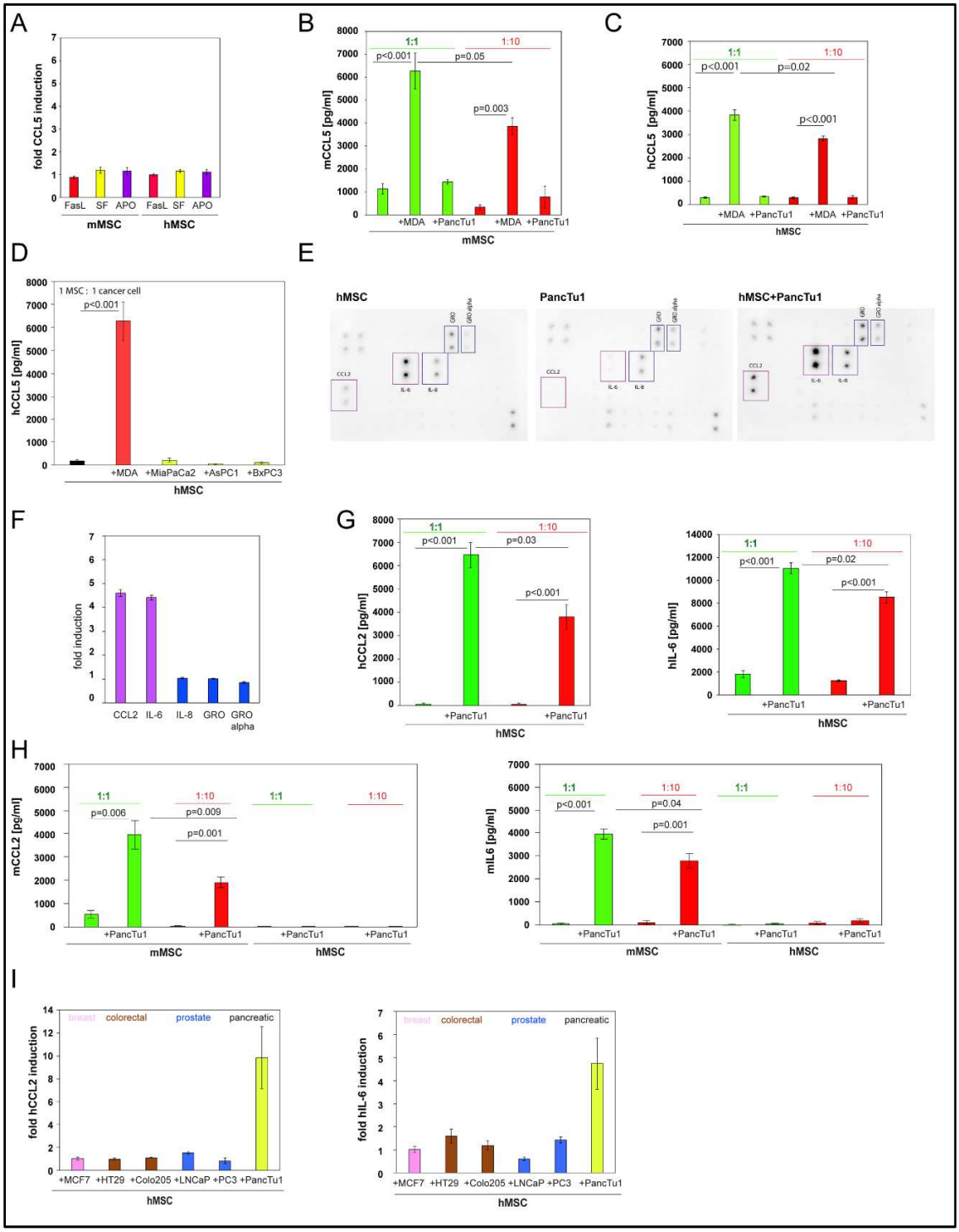

Figure 3. Pancreatic cancer cells stimulate MSCs to produce the pro-metastatic cytokines CCL2 and IL6.

(A) Murine (mMSC) and human MSCs (hMSC) were treated with 0.2 ng/ml FasL, 0.2 ng/ml multimeric-FasL (SF) and 0.2 ng/ml of an anti-APO-1-3 antibody (APO) for 72 hours. The resulting supernatants were analysed for CCL5 by ELISA. Results are the mean ± SEM; n=3.

(B) Murine MSCs (mMSCs) were mixed with MDA-MB-231 (MDA) and PancTu1 cells at ratios of 1:1 and 1:10. The resulting supernatants were analysed for CCL5 by ELISA. Results are the mean ± SEM; n=3.

(C) Human MSCs (hMSCs) were mixed with MDA-MB-231 (MDA) and PancTu1 cells at ratios of 1:1 and 1:10. The resulting supernatants were analysed for CCL5 by ELISA. Results are the mean ± SEM; n=3.

(D) Human MSCs (hMSCs) were mixed with three different pancreatic cancer cell lines (MiaPaCa2, AsPC1 and BxPC3) at a ratio of 1:1 and the resulting supernatants analysed for CCL5 by ELISA. Mixing experiments with MDA-MB-231 (MDA) cells were carried out as positive control. Results are the mean ± SEM; n=3.

(E) Human MSCs (hMSCs) were mixed with PancTu1 cells at a ratio of 1:10 for 48 hours and the supernatant applied to a cytokine antibody array (right). Supernatants from hMSCs (left) and PancTu1 cells (centre), respectively, were used as controls.

(F) Quantification of selected cytokines (boxed-in in Figure 3E) from the cytokine antibody array.

(G) Human MSCs (hMSCs) were mixed with PancTu1 cells at ratios of 1:1 and 1:10. The resulting supernatants were analysed for CCL2 (left) and IL6 (right) by ELISA. Results are the mean ± SEM; n=3.

(H) Murine MSCs (mMSCs) and human MSCs (hMSCs) were mixed with PancTu1 cells at ratios of 1:1 and 1:10. The resulting supernatants were analysed for CCL2 (left) and IL6 (right) using murine-specific ELISAs. Results are the mean ± SEM; n=3.

(I) Human MSCs (hMSCs) were mixed with different cancer cell lines (MCF7, HT29, Colo205, LNCaP, PC3) at a ratio of 1:1. The resulting supernatants were analysed for CCL2 (left) and IL6 (right) by ELISA. PancTu1 cells were used as positive controls. Results are the mean ± SEM; n=3 (CCL2); n=4 (IL6).

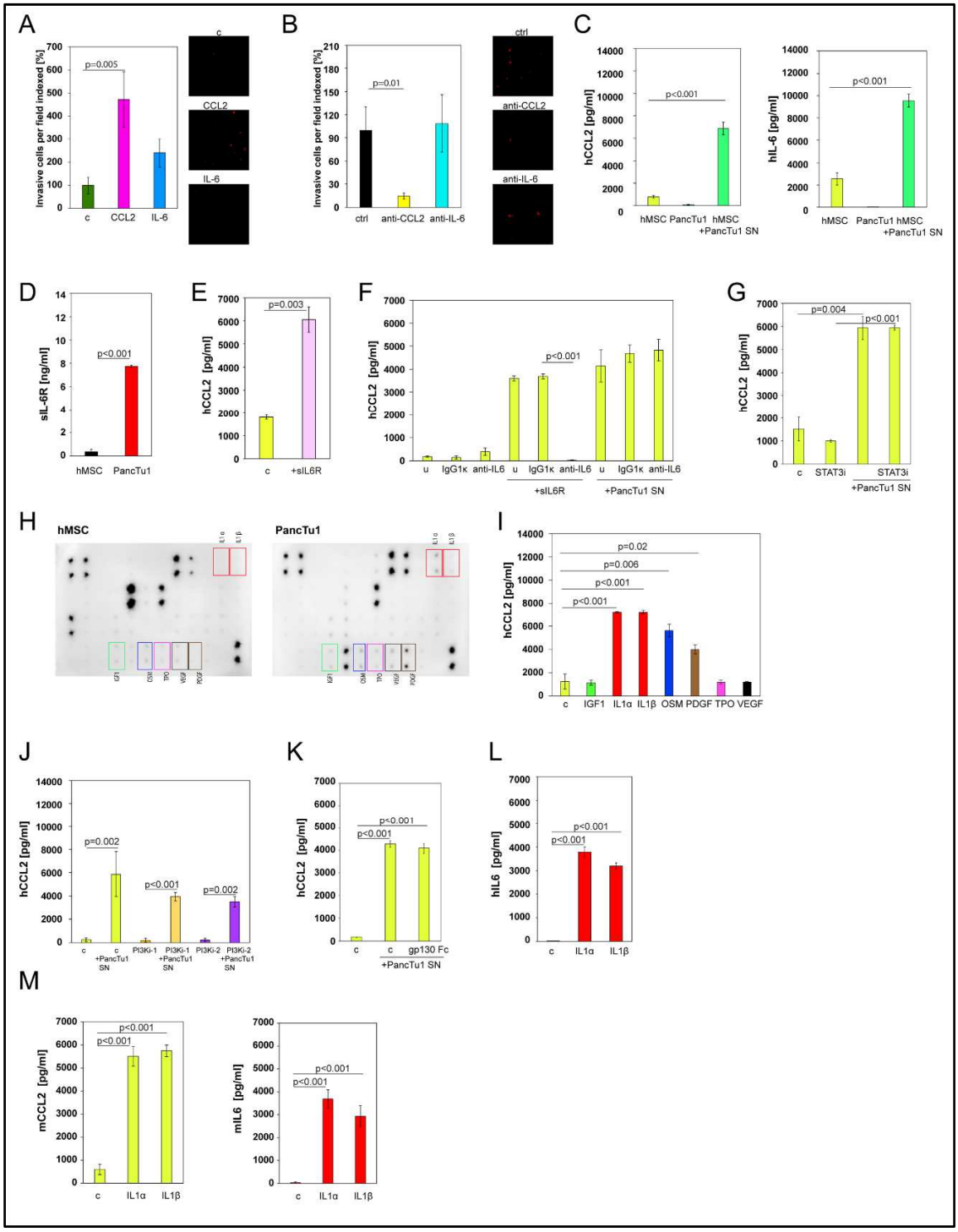

Figure 4. A pancreatic cancer cell-derived soluble factor is responsible for the induction of CCL2 and IL6 in MSCs.

(A) CM-Dil labelled PancTu1 cells were cultured in the presence of carrier (c), CCL2 or IL6 in the upper well of Boyden chambers. Representative images (right) show the labelled PancTu1 cells that migrated through Matrigel coated membranes in 72 hours. Quantification of the migration activity of the cells is shown on the left. Results are the mean ± SEM of 5 randomly chosen fields per experiment; n=3.

(B) CM-Dil labelled PancTu1 cells were cultured in the presence of human MSCs with anti-CCL2, anti-IL6 or a control (ctrl) antibody in the upper wells of Boyden chambers. Representative images (right) show the labelled PancTu1 cells that migrated through Matrigel coated membranes in 72 hours. Quantification of the migration activity of the cells is shown on the left. Results are the mean ± SEM of 5 randomly chosen fields per experiment; n=2.

(C) CCL2 (left) and IL6 (right) ELISAs of supernatants from human MSCs (hMSCs) that were treated with conditioned medium of PancTu1 cells (SN) for 72 hours. Supernatants of PancTu1 cells and MSCs are shown as controls. Results are the mean ± SEM; n=3.

(D) ELISA for sIL6R of supernatants from human MSCs (hMSCs) and PancTu1 cells. Results are the mean ± SEM; n=3.

(E) CCL2 ELISA of human MSC supernatants after treatment with recombinant sIL6R for 72 hours. Carrier controls (c) are depicted as controls. Results are the mean ± SEM; n=3.

(F) CCL2 ELISA of supernatants from human MSCs treated with conditioned medium of PancTu1 cells (SN) supplemented with neutralising antibodies against IL6. IgG1κ antibodies and MSCs treated with recombinant sIL6R were used as controls. The results of untreated samples (u) are also shown. Results are the mean ± SEM; n=3.

(G) CCL2 ELISA of supernatants from human MSCs treated with conditioned medium of PancTu1 cells (SN) and a STAT3 inhibitor (STATi). Carrier-treated MSCs (c) and MSCs treated with STAT3 inhibitor alone are shown as controls. Results are the mean ± SEM; n=3.

(H) Long exposure images of cytokine antibody arrays probed with supernatants of human MSCs (hMSCs) and PancTu1 cells, respectively. Differentially expressed growth factors and cytokines are highlighted.

(I) CCL2 ELISA of supernatants from human MSCs treated with different recombinant cytokines (IGF1, IL1α, IL1β, OSM, PDGF, TPO and VEGF). Carrier-treated controls (c) are also shown. Results are the mean ± SEM; n=3.

(J) CCL2 ELISA of supernatants from human MSCs treated with conditioned medium from PancTu1 cells (SN) in the presence of two different PI3K inhibitors. Carrier-treated MSCs (c) and inhibitors alone were used as controls. Results are the mean ± SEM; n=3.

(K) CCL2 ELISA of supernatants from human MSCs treated with conditioned medium from PancTu1 cells (SN) and gp130-Fc. Carrier-treated MSCs (c) are shown as controls. Results are the mean ± SEM; n=3.

(L) IL6 ELISA of supernatants from human MSCs treated with IL1α and IL1β. A carrier control (c) is also depicted in the graph. Results are the mean ± SEM; n=3.

(M) CCL2 (left) and IL6 (right) ELISAs of supernatants from murine MSCs treated with IL1α and IL1β. Carrier controls (c) are also depicted in the graphs. Results are the mean ± SEM; n=3.

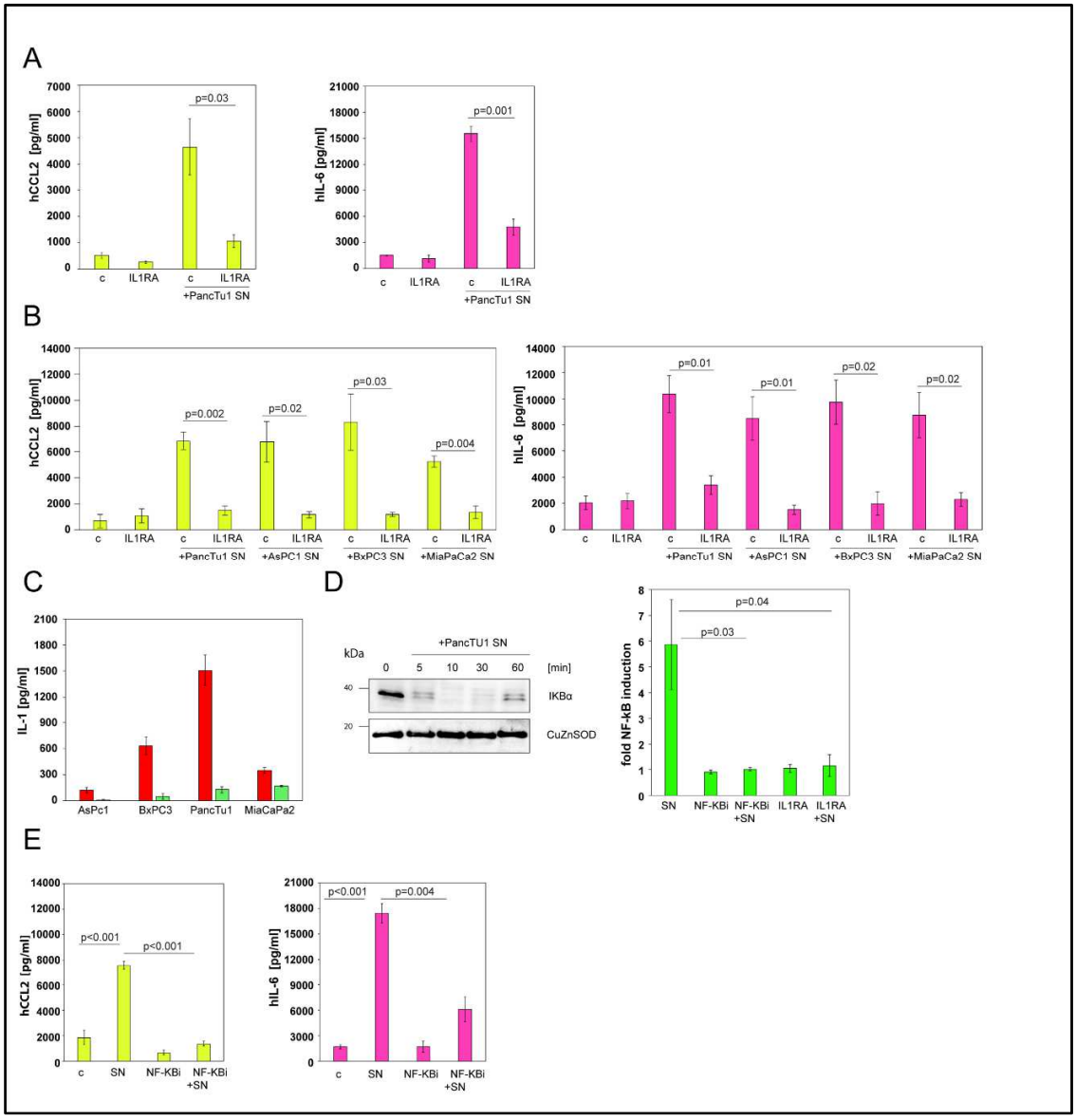

Figure 5. Pancreatic cancer-derived IL1 induces CCL2 and IL6 via NF-κB activation in MSCs.

(A) CCL2 (left) and IL6 (right) ELISAs of supernatants from human MSCs treated with conditioned medium (SN) from PancTu1 cells in the presence of IL1RA. Carrier controls (c) and MSCs treated with IL1RA alone are also depicted in the graphs. Results are the mean ± SEM; n=3.

(B) CCL2 (left) and IL6 (right) ELISAs of supernatants from human MSCs treated with conditioned medium (SN) from different pancreatic cancer cell lines (PancTu1, AsPC1, BxPC3, MiaPaCa) in the presence of IL1RA. Carrier controls (c) are also shown in the graphs. Results are the mean ± SEM; n=3.

(C) IL1α (red) and IL1β (green) ELISAs of supernatants from different pancreatic cancer cell lines (AsPC1, BxPC3, PancTu1, MiaPaCa). Results are the mean ± SEM; n=4.

(D) Western blot (left) of IκBα of human MSCs treated with conditioned medium from PancTu1 cells for different time points (0, 5, 10, 30, 60 min). The CuZnSOD blot serves as loading control. NF-κB reporter assay results (right) of MSCs treated with conditioned medium from PancTu1 cells (SN) as well as MSCs pre-treated with an NF-κB inhibitor (NF-κBi) and IL1RA, respectively. MSCs treated with NF-κB inhibitor or IL1RA alone were used as controls. Results are the mean ± SEM; n=4.

(E) CCL2 (left) and IL6 (right) ELISAs of supernatants from human MSCs treated with conditioned medium from PancTu1 cells (SN) with and without NF-κB inhibitor (NF-κBi). MSCs treated with carrier (c) or NF-κB inhibitor alone are shown as controls. Results are the mean ± SEM; n=3.

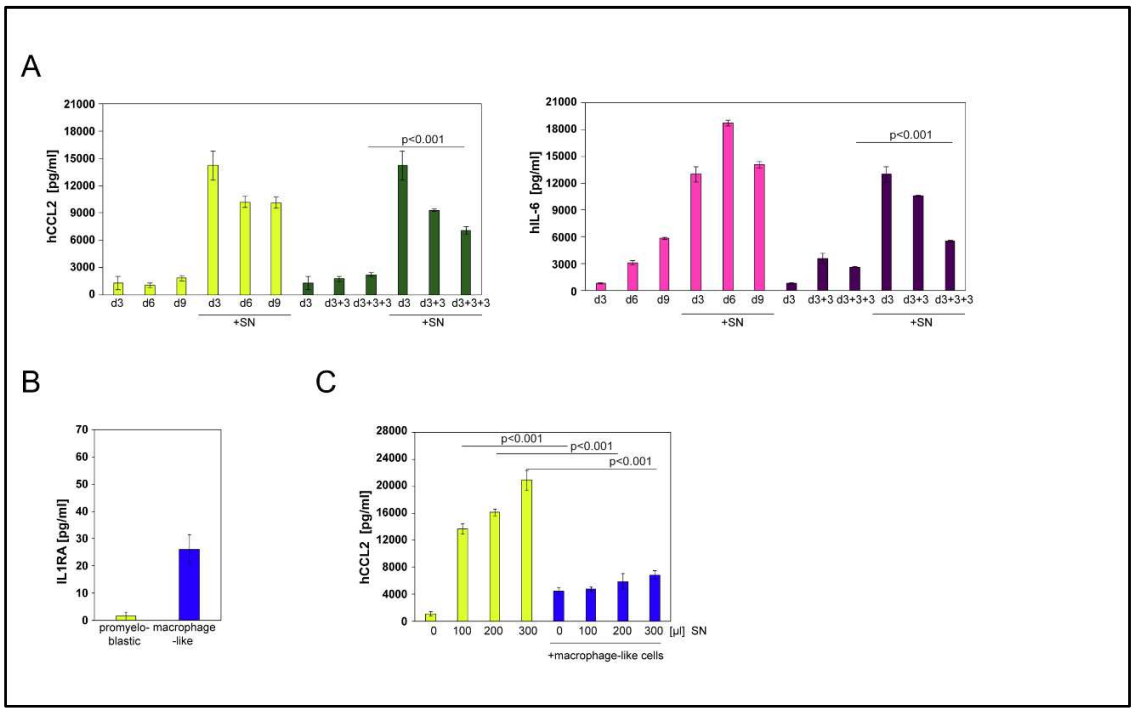

Figure 6. IL1 gives rise to sustained CCL2 and IL6 production in MSCs and monocytic cells inhibit the induction of the two cytokines.

(A) CCL2 (left) and IL6 (right) ELISAs of supernatants from human MSCs treated with conditioned medium from PancTu1 cells (SN) for three days followed by medium change every three days (dark green/purple bars). In comparison MSCs treated with conditioned medium from PancTu1 cells (SN) without medium change are shown (yellow/pink bars). MSCs without addition of conditioned medium serve as controls. Results are the mean ± SEM; n=3.

(B) IL1RA ELISA of supernatants of pro-myeloblastic and differentiated, macrophage-like cells. Results are the mean ± SEM; n=3.

(C) CCL2 ELISA of supernatants from human MSCs treated with different amounts of conditioned medium from PancTu1 cells (SN) in the presence of macrophage-like cells (blue bars). Supernatants from MSCs treated with different amounts of conditioned

medium without macrophage-like cells are depicted as controls (yellow bars). Results are the mean ± SEM; n=3.

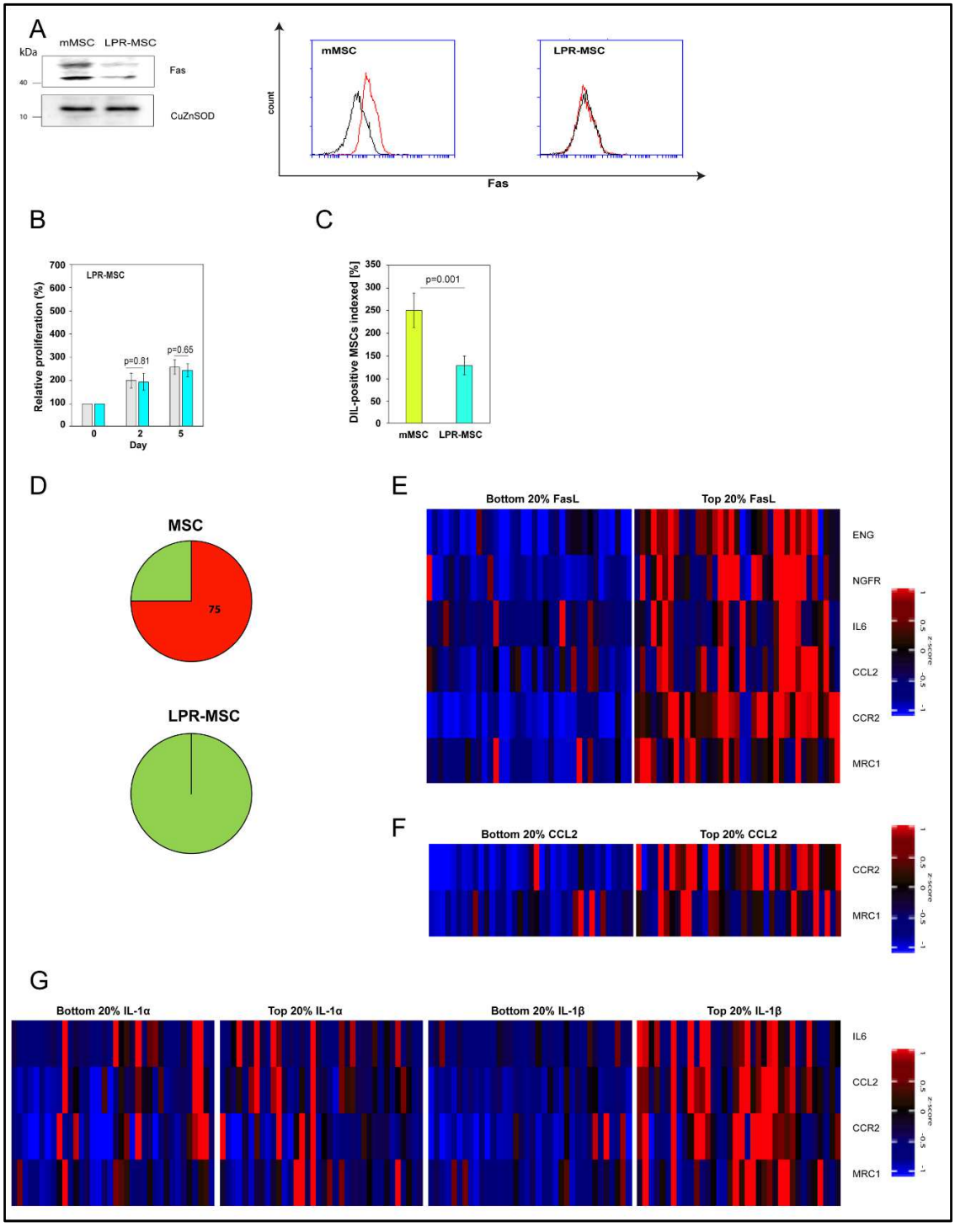

Figure 7. Fas-deficient MSCs do not promote metastasis development.

(A) Western blot (left) for Fas expression in murine MSCs (mMSCs) and LPR-MSCs. The CuZnSOD blot serves as loading control. Flow cytometric analysis (right) of Fas surface

expression (red) on murine MSCs (mMSCs) and LPR-MSCs. The isotype control is shown in black.

(B) LPR-MSCs were treated with 0.2 ng/ml of FasL for 2 and 5 days and cell numbers determined (turquoise). MSCs treated with carrier are shown as controls (grey). The numbers of LPR-MSCs at the start of FasL treatment (Day 0) were set to 100%. Results are the mean ± SEM; n=6.

(C) Relative numbers of murine MSCs (mMSCs) and LPR-MSCs found in tumour-burdened (PancTu1) animals after 28 days. Each cohort consisted of four animals.

(D) Incidence of lung metastases in PancTu1 tumour-burdened animals after systemic administration of murine MSCs (mMSCs) or LPR-MSCs. Each cohort consisted of four animals.

(E) Heatmap of MSC-markers (ENG, NGFR), cytokines (IL6, CCL2) and monocytic markers (CCR2, MRC1) that are significantly co-expressed ($p \leq 0.001$) with FasL. The heatmap shows 20% of samples with highest and lowest FasL expression, respectively. n=186.

(F) Heatmap of monocytic markers (CCR2, MRC1) significantly co-expressed ($p \leq 0.001$) with CCL2 showing 20% of samples with highest and lowest CCL2 expression, respectively. n=186.

(G) Heatmap of cytokines (IL6, CCL2) and monocytic markers (CCR2, MRC1) that are co-expressed with IL1α (left) and IL1β (right; $p \leq 0.001$) showing 20% of samples with highest and lowest IL1α/IL1β expression, respectively. n=186.

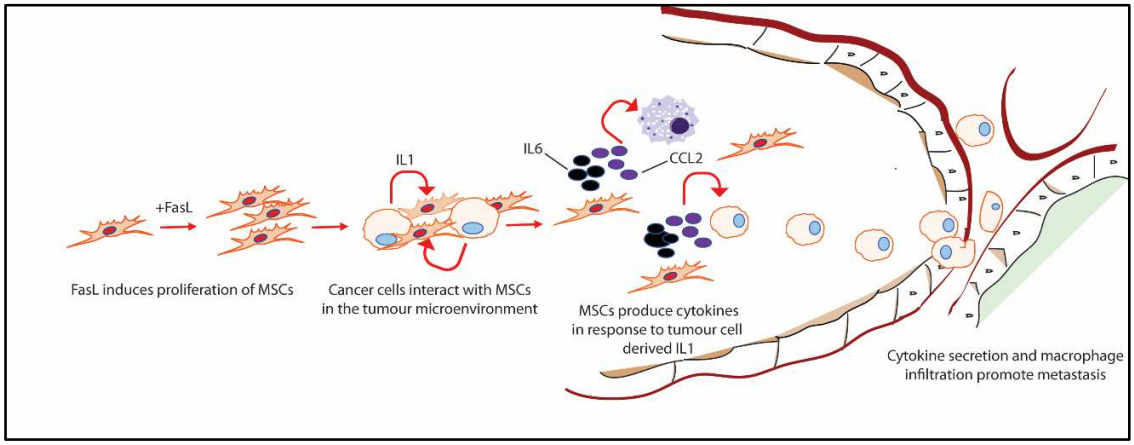

Figure 8. Schematic diagram of FasL-induced mechanism

Model of the effect of FasL on MSCs and their role in the crosstalk with pancreatic cancer cells in the TME.

Supplementary Figures and Legends

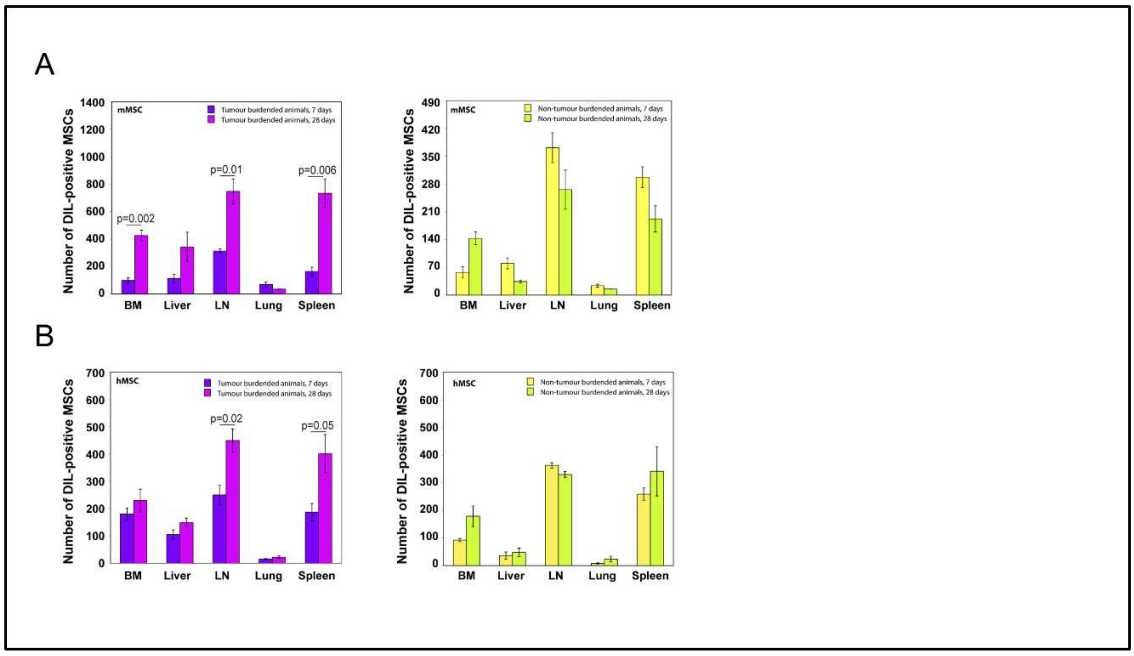

Supplementary Figure 1

(A) Quantification of the total number of murine MSCs (mMSCs) in different tissues of tumour-bearing mice after 7 days (purple) and after 28 days (pink). Quantification of the total number of murine MSCs (mMSCs) in non-tumour-bearing mice after 7 days (yellow) and after 28 days (green).

(B) Quantification of the total number of human MSCs (hMSCs) in different tissues of tumour-bearing mice after 7 days (purple) and after 28 days (pink). Quantification of the total number of human MSCs (hMSCs) in non-tumour-bearing mice after 7 days (yellow) and after 28 days (green).

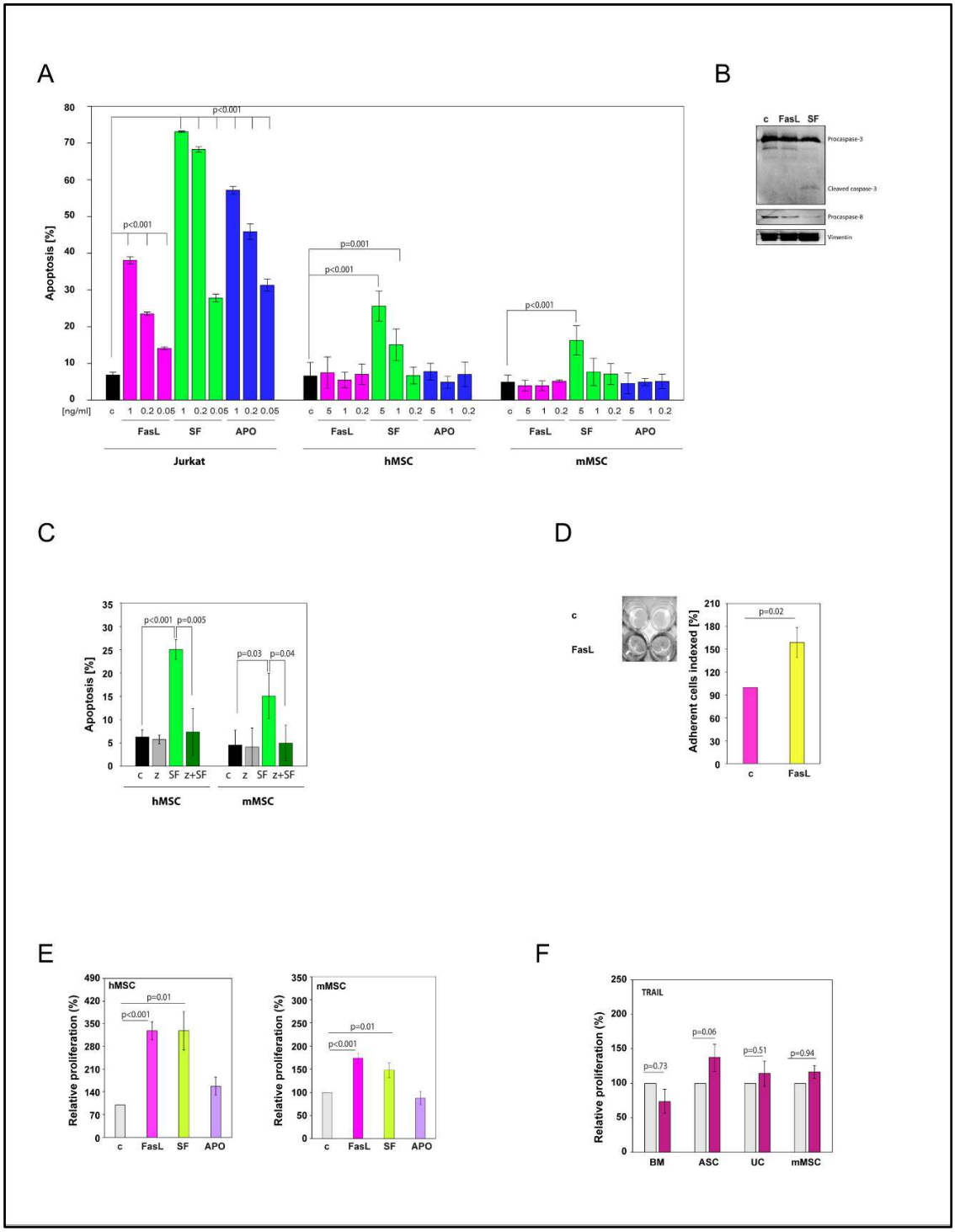

Supplementary Figure 2

(A) Apoptosis measurements in Jurkat cells, human MSCs (hMSCs) and murine MSCs (mMSCs) after treatment with FasL, multimeric-FasL (SF) and anti-APO-1-3 (APO) for

24 h, at concentrations ranging from 0.05-5 ng/ml. Controls (c) were treated with carrier only. Results are the mean ± SEM; n=3 (Jurkat), n=6 (MSCs).

(B) Western blot of Caspase-3 and Caspase-8 on protein lysates from human MSCs (hMSCs) treated with 5 ng/ml FasL or 5 ng/ml multimeric-FasL (SF). Vimentin served as loading control.

(C) Human MSCs (hMSCs) and murine MSCs (mMSCs) were pre-treated with 20 μM zVAD (z) ± 5 ng/ml multimeric-FasL (SF). Apoptosis was measured after 24 h. Controls (c) were treated with carrier only. Results are the mean ± SEM; n=3.

(D) Growth of human MSCs following treatment with carrier (c) or 0.2 ng/ml of FasL for 5 days. The cells were visualized by crystal violet stain. A representative image is shown on the left and quantification of the results on the right. Growth of the untreated cells after 5 days was set to 100%. Results are the mean ± SEM; n=5.

(E) Human MSCs (hMSCs; left) and murine MSCs (mMSCs; right) were treated with FasL, multimeric-FasL (SF) and anti-APO-1-3 (APO) as shown in the figure for 2 days. The numbers of MSCs in the carrier controls (c) were set to 100%. Results are the mean ± SEM; n=4 (hMSC); n=8 (mMSC).

(F) Human MSCs from bone marrow (BM), adipose tissue (ASC) and umbilical cord (UC) as well as murine MSCs (mMSC) were treated with 0.2 ng/ml of TRAIL for 2 days and cell numbers determined (purple). MSCs treated with carrier are shown as controls (grey). The numbers of MSCs at the start of TRAIL treatment were set to 100%. Results are the mean ± SEM; (n=4).

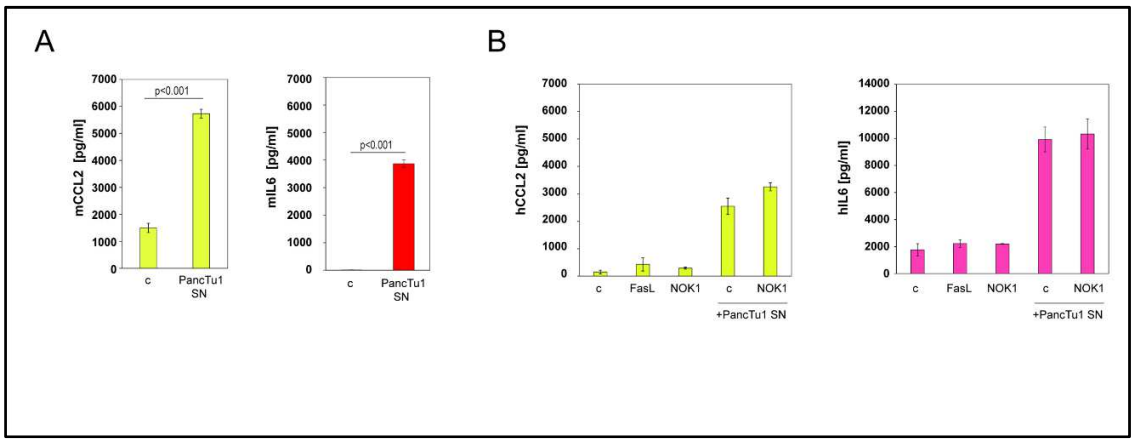

Supplementary Figure 3

(A) CCL2 (left) and IL6 (right) ELISAs of supernatants from murine MSCs (mMSCs) treated with conditioned medium from PancTu1 cells (SN) for 48 h. MSCs treated with unconditioned medium served as controls (c). Results are the mean ± SEM; n=3.

(B) CCL2 (left) and IL6 (right) ELISAs of supernatants from human MSCs (hMSCs) treated with 0.2 ng/ml FasL or 2.5 µg/ml NOK-1 antibody ± conditioned medium from PancTu1 cells (SN) for 48 h. MSCs treated with carrier served as controls (c). Results are the mean ± SEM; n=3.

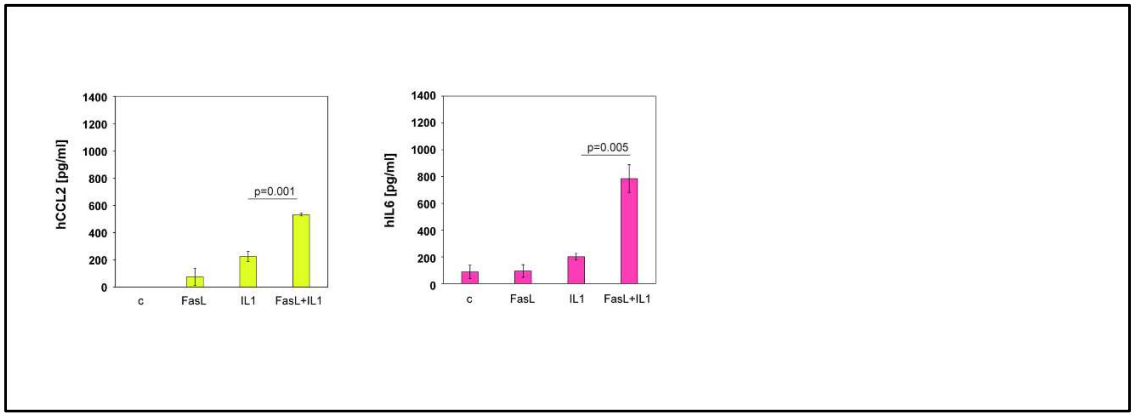

Supplementary Figure 4

CCL2 (left) and IL6 (right) ELISAs of supernatants from human MSCs (hMSCs) treated with 0.2 ng/ml FasL for three days in medium containing 1% FCS, followed by 50 ng/ml IL1α for 48 h. MSCs treated with carrier served as controls (c). Results are the mean ± SEM; n=3.

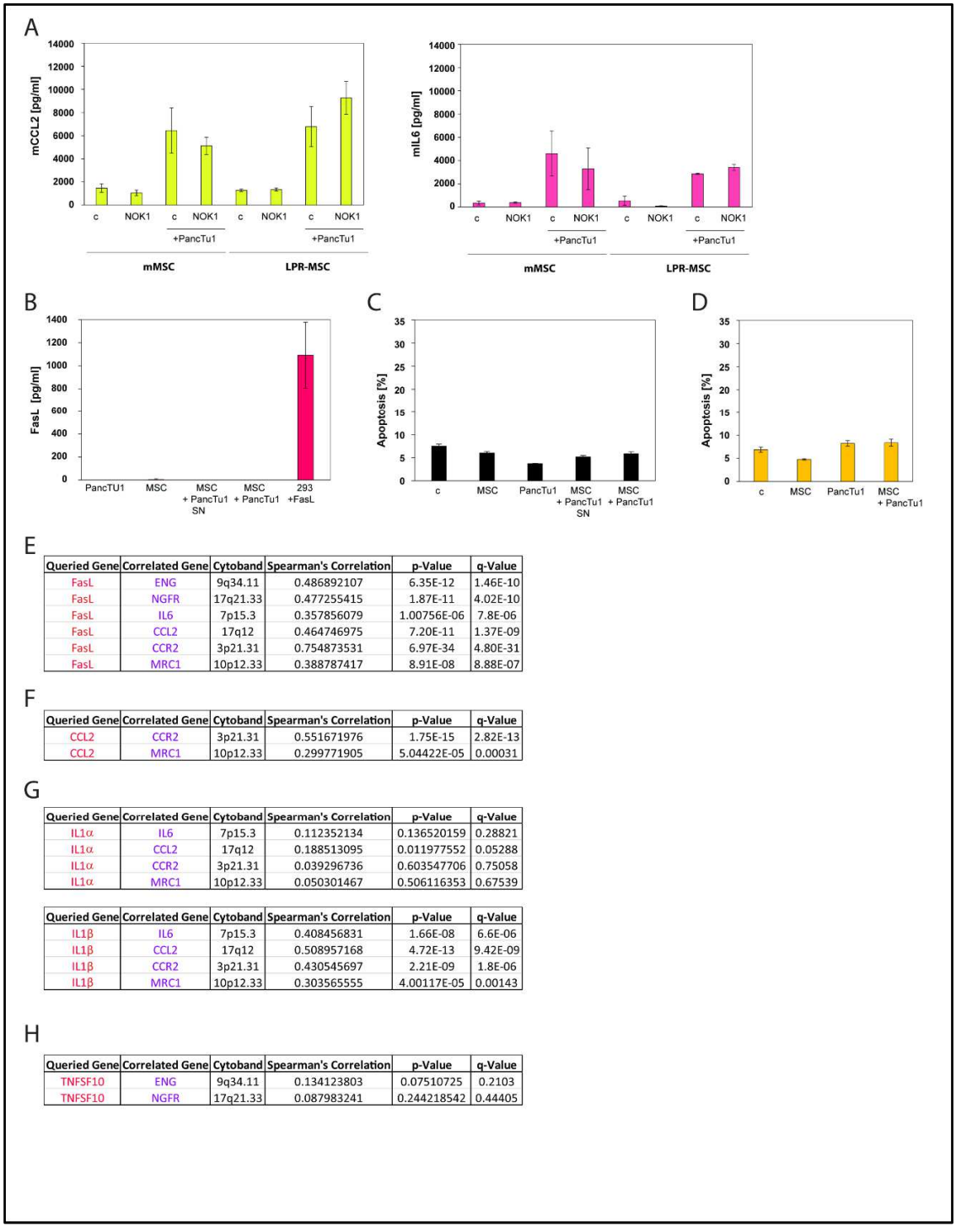

E

Queried Gene	Correlated Gene	Cytoband	Spearman's Correlation	p-Value	q-Value
FasL	ENG	9q34.11	0.486892107	6.35E-12	1.46E-10
FasL	NGFR	17q21.33	0.477255415	1.87E-11	4.02E-10
FasL	IL6	7p15.3	0.357856079	1.00756E-06	7.8E-06
FasL	CCL2	17q12	0.464746975	7.20E-11	1.37E-09
FasL	CCR2	3p21.31	0.754873531	6.97E-34	4.80E-31
FasL	MRC1	10p12.33	0.388787417	8.91E-08	8.88E-07

F

Queried Gene	Correlated Gene	Cytoband	Spearman's Correlation	p-Value	q-Value
CCL2	CCR2	3p21.31	0.551671976	1.75E-15	2.82E-13
CCL2	MRC1	10p12.33	0.299771905	5.04422E-05	0.00031

G

Queried Gene	Correlated Gene	Cytoband	Spearman's Correlation	p-Value	q-Value
IL1α	IL6	7p15.3	0.112352134	0.136520159	0.28821
IL1α	CCL2	17q12	0.188513095	0.011977552	0.05288
IL1α	CCR2	3p21.31	0.039296736	0.603547706	0.75058
IL1α	MRC1	10p12.33	0.050301467	0.506116353	0.67539

Queried Gene	Correlated Gene	Cytoband	Spearman's Correlation	p-Value	q-Value
IL1β	IL6	7p15.3	0.408456831	1.66E-08	6.6E-06
IL1β	CCL2	17q12	0.508957168	4.72E-13	9.42E-09
IL1β	CCR2	3p21.31	0.430545697	2.21E-09	1.8E-06
IL1β	MRC1	10p12.33	0.303565555	4.00117E-05	0.00143

H

Queried Gene	Correlated Gene	Cytoband	Spearman's Correlation	p-Value	q-Value
TNFSF10	ENG	9q34.11	0.134123803	0.07510725	0.2103
TNFSF10	NGFR	17q21.33	0.087983241	0.244218542	0.44405

Supplementary Figure 5

(A) CCL2 (left) and IL6 (right) ELISAs of supernatants from murine MSCs (mMSCs) and LPR-MSCs ± PancTu1 cells (at a ratio of 1:1) and ± 2.5 µg/ml NOK-1 antibody for 48 h. MSCs treated with carrier served as controls (c). Results are the mean ± SEM; n=3.

(B) FasL ELISA of supernatants from human MSCs (hMSCs), PancTu1 cells, hMSCs treated with conditioned medium from PancTu1 cells and hMSCs mixed with PancTu1 cells (at a ratio of 1:1) for 48 h. HEK293 cells, transiently transfected with a hFasL (293+FasL) expression construct, were used as positive control. Results are the mean ± SEM; n=3.

(C) Apoptosis measurements of Jurkat cells treated with supernatants from human MSCs (hMSCs), PancTu1 cells, hMSCs treated with conditioned medium from PancTu1 cells and hMSCs mixed with PancTu1 cells (at a ratio of 1:1) for 48 h. Results are the mean ± SEM; n=3.

(D) Apoptosis measurements of Jurkat cells co-cultured with human MSCs (hMSCs), PancTu1cells and a combination of PancTu1 cells and hMSCs. Apoptosis was measured after 48 h. Results are the mean ± SEM; n=3.

(E) Correlation coefficients and p-values of co-expression relationships of FasL with the listed genes.

(F) Correlation coefficients and p-values of co-expression relationships of CCL2 with the listed genes.

(G) Correlation coefficients and p-values of co-expression relationships of IL1α (top) and IL1β (bottom) with the listed genes.

(H) Correlation coefficients and p-values of co-expression relationships of TNFSF10 (TRAIL) with the listed genes.